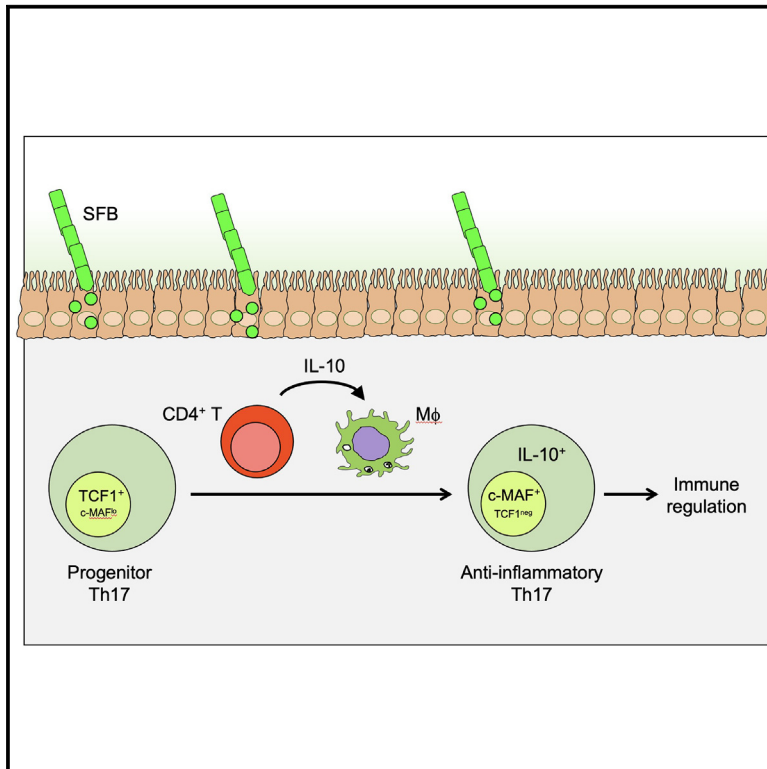


Immunity

Intestinal microbiota-specific Th17 cells possess regulatory properties and suppress effector T cells via c-MAF and IL-10

Graphical abstract



Authors

Leonie Brockmann, Alexander Tran, Yiming Huang, Madeline Edwards, Carlotta Ronda, Harris H. Wang, Ivaylo I. Ivanov

Correspondence

ii2137@cumc.columbia.edu

In brief

The function of commensal-specific Th17 cells in host homeostasis is unclear. Brockmann et al. report that tissue-resident commensal-induced Th17 cells have an anti-inflammatory phenotype and can regulate effector T cell responses. Anti-inflammatory Th17 cells are sustained locally from a resident gut TCF1⁺ progenitor population and signals from intestinal macrophages.

Highlights

- SFB-specific Th17 cells have anti-inflammatory phenotype driven by c-MAF and IL-10
- Commensal-induced Th17 cells regulate T cell activity in an IL-10-dependent manner
- TCF1⁺ progenitor Th17 cells generate IL-10⁺ SFB-induced Th17 cells locally in the gut
- IL-10 signaling in gut macrophages drives anti-inflammatory Th17 cell phenotype

Article

Intestinal microbiota-specific Th17 cells possess regulatory properties and suppress effector T cells via c-MAF and IL-10

Leonie Brockmann,¹ Alexander Tran,¹ Yiming Huang,^{2,3} Madeline Edwards,¹ Carlotta Ronda,³ Harris H. Wang,^{3,4} and Ivaylo I. Ivanov^{1,5,*}

¹Department of Microbiology and Immunology, Vagelos College of Physicians and Surgeons, Columbia University, New York, NY 10032, USA

²Integrated Program in Cellular, Molecular, and Biomedical Studies, Columbia University, New York, NY 10032, USA

³Department of Systems Biology, Vagelos College of Physicians and Surgeons, Columbia University, New York, NY 10032, USA

⁴Department of Pathology and Cell Biology, Vagelos College of Physicians and Surgeons, Columbia University, New York, NY 10032, USA

⁵Lead contact

*Correspondence: ii2137@cumc.columbia.edu

<https://doi.org/10.1016/j.immuni.2023.11.003>

SUMMARY

Commensal microbes induce cytokine-producing effector tissue-resident CD4⁺ T cells, but the function of these T cells in mucosal homeostasis is not well understood. Here, we report that commensal-specific intestinal Th17 cells possess an anti-inflammatory phenotype marked by expression of interleukin (IL)-10 and co-inhibitory receptors. The anti-inflammatory phenotype of gut-resident commensal-specific Th17 cells was driven by the transcription factor c-MAF. IL-10-producing commensal-specific Th17 cells were heterogeneous and derived from a TCF1⁺ gut-resident progenitor Th17 cell population. Th17 cells acquired IL-10 expression and anti-inflammatory phenotype in the small-intestinal lamina propria. IL-10 production by CD4⁺ T cells and IL-10 signaling in intestinal macrophages drove IL-10 expression by commensal-specific Th17 cells. Intestinal commensal-specific Th17 cells possessed immunoregulatory functions and curbed effector T cell activity *in vitro* and *in vivo* in an IL-10-dependent and c-MAF-dependent manner. Our results suggest that tissue-resident commensal-specific Th17 cells perform regulatory functions in mucosal homeostasis.

INTRODUCTION

Mucosal surfaces are colonized by a vast collection of resident microorganisms that shape tissue immune responses.^{1,2} Intestinal tolerance toward commensals is promoted by induction of commensal-specific Foxp3⁺ regulatory T (Treg) cells.^{3–5} However, commensals can also induce effector CD4⁺ T cells, such as interleukin (IL)-17-producing CD4⁺ T cells (T helper 17 [Th17] cells).^{6–9} The functions of commensal-specific Th17 cells (hereafter referred to as commensal Th17 cells) in mucosal immunity are incompletely understood. They can contribute to control of the inducing commensal,¹⁰ but whether they perform additional functions in mucosal homeostasis is unclear.

Th17 cells are a functionally heterogeneous population and can acquire pathogenic and non-pathogenic phenotypes.^{11–15} Th17 cells are known drivers of inflammation, including intestinal inflammation, and can promote the pathology of inflammatory bowel diseases (IBDs).^{16,17} However, not all Th17 cells are inflammatory. For example, Th17 cell-derived cytokines participate in strengthening the epithelial barrier and, therefore, counteract inflammation.^{18–21} Th17 cells can also produce IL-10 and intestinal Th17 cells can convert to a regulatory phenotype under

inflammatory conditions.^{12,15,22} Although inflammatory Th17 cells have been well studied, the functions of non-pathogenic Th17 cells are incompletely understood.²³

Gut-resident commensal Th17 cells are metabolically distinct from inflammatory Th17 cells²⁴ and are generally considered non-pathogenic. However, whether commensal Th17 cells simply fail to participate in inflammatory responses or possess specific effector mechanisms to regulate inflammation that may direct additional functions in mucosal homeostasis is currently unknown.

Here, we examine in more detail the phenotype of various types of intestinal Th17 cells, including commensal Th17 cells induced by segmented filamentous bacteria (SFB). We find that SFB Th17 cells possess unique anti-inflammatory phenotype characterized by expression of the transcription factor c-MAF and the cytokine IL-10. Establishment of this program occurs in the terminal ileum and requires the coordinated action of intestinal CD4⁺ T cells and intestinal macrophages (iM ϕ). We also find that SFB Th17 cells can curb effector T cell function both *in vitro* and *in vivo*. Our results describe anti-inflammatory functions of commensal Th17 cells and suggest that these cells may have important roles in maintaining intestinal homeostasis.

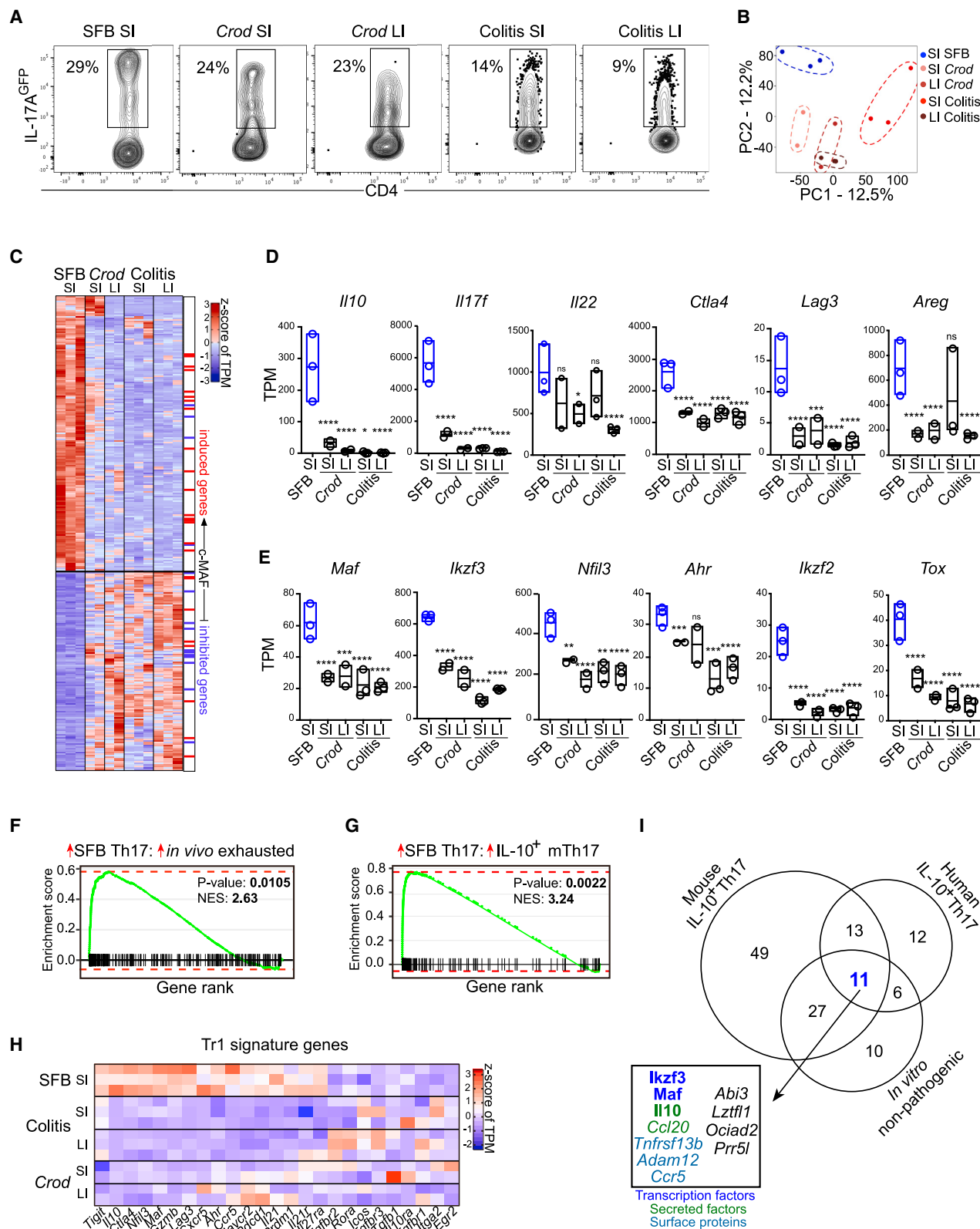


Figure 1. SFB Th17 cells have an anti-inflammatory transcriptional program

(A) Intestinal lamina propria (LP) Th17 cells induced by various mechanisms. SI, small intestine; LI, large intestine; colitis, CD45RB^{hi} colitis. Representative fluorescence-activated cell sorting (FACS) plots gated on TCRβ⁺CD4⁺ LP lymphocytes.

(legend continued on next page)

RESULTS

Small-intestinal commensal Th17 cells have a regulatory transcriptional program

To identify unique features of commensal Th17 cells, we profiled their transcriptome by RNA sequencing (RNA-seq) and compared it with the transcriptome of alternatively generated intestinal Th17 cells. *Il17a^{GFP}* reporter animals were colonized with SFB to induce commensal Th17 cells (SFB Th17 cells). Intestinal Th17 cells were also induced by infecting *Il17a^{GFP}* animals with *Citrobacter rodentium* (*Crod*) or by transferring naive CD45RB^{hi} CD4⁺ T cells from *Il17a^{GFP}* animals into RAG1-deficient animals in a classical model of intestinal inflammation. Lamina propria (LP) Th17 cells were isolated from small (SI) and large (LI) intestine at the peak of microbial colonization or colitis induction (Figures S1A–S1C). Th17 cells comprised large percentage of CD4⁺ T cells in intestinal tissues (Figure 1A). However, Th17 cell phenotype differed between different conditions (Figure 1B). The transcriptional program of SFB-induced Th17 cells was distinct from the transcriptional programs of other intestinal Th17 cells (Figure 1B). Expression of 500–1,100 genes differed between SFB Th17 cells and any other examined intestinal Th17 cells (Figures S1D and S1E). In contrast, differentially expressed gene (DEG) numbers were lower in pairwise comparisons between non-SFB Th17 cells (Figure S1E). We identified a core signature of 309 DEGs between SFB Th17 cells and at least three of the other Th17 cell datasets (Figures 1C and S1F). The core SFB Th17 cell program contained genes involved in inhibitory/regulatory (e.g., *Ctla4*, *Lag3*, and *Tigit*), anti-inflammatory (e.g., *Maf* and *Il10*) and tissue-protective (e.g., *Ahr* and *Areg*) functions (Figures 1D, 1E, and S1G). At the same time, genes enriched in inflammatory Th17 cells were underrepresented in SFB Th17 cells (Figure S1H). Overall, SFB Th17 cells specifically expressed genes associated with decreased T cell responsiveness.²⁵ We, therefore, compared this program with the gene signatures of “non-responsive” T cells, such as exhausted and Treg cells. SFB Th17 cells resembled exhausted CD4⁺ T cells generated following chronic infection²⁶ (Figure 1F) and expressed classical markers of CD4⁺ T cell exhaustion such as *Ikzf2* and *Tox*^{27,28} (Figure 1E). At the same time, SFB Th17 cells closely resembled mouse and human IL-10 expressing immunoregulatory Th17 cells^{12,29} (Figures 1G and S1I). Moreover, commensal-induced Th17 cells were enriched in a subset of signature genes for IL-10⁺Foxp3⁻ type 1 regulatory (Tr1) cells (Figure 1H). Comparison of core leading-edge genes in SFB Th17 cells to published mouse and human IL-10-expressing Th17 cells and non-pathogenic Th17 cells identified a set of 11 common genes, including genes encoding the prototypical anti-inflammatory cytokine IL-10, and the transcription factor

c-MAF^{30–32} (Figure 1I). Among intestinal Th17 cells, expression of *Il10* transcripts was restricted to commensal Th17 cells (Figures 1D and S1G) and *Maf* expression was elevated in SFB Th17 cells (Figures 1E and S1G). In addition to *Maf*, several other transcription factors, including *Maf* co-factors, involved in regulation of *Il10* in CD4⁺ T cells, such as *Ikzf3*, *Ahr* and *Nfil3*^{33–35} were also expressed preferentially in commensal intestinal Th17 cells (Figure 1E). Collectively, these results suggest that commensal intestinal Th17 cells possess an anti-inflammatory transcriptional program that resembles that of IL-10-producing regulatory CD4⁺ T cells.

Small-intestinal commensal Th17 cells express IL-10 and co-inhibitory receptors

To confirm the RNA-seq data, we followed expression of IL-10 in commensal or non-commensal Th17 cells using *Il10^{GFP}/Il17a^{Katushka}/Foxp3^{mRFP}* reporter mice. Non-commensal Th17 cells lacked expression of IL-10 in SI and LI LP (Figures 2A, 2B, and S2A). In contrast, ~40% of SFB-induced Th17 cells in the SI co-expressed IL-17 and IL-10 (Figures 2A and 2B). *Citrobacter*-induced and colitogenic intestinal Th17 cells produced interferon (IFN)- γ and granulocyte-macrophage colony-stimulating factor (GM-CSF) (Figures S2B and S2C). In contrast, commensal Th17 cells lacked expression of these inflammatory cytokines (Figures S2B and S2C). We also examined expression of c-MAF in intestinal Th17 cells by flow cytometry. SFB colonization increased the proportion of Th17 cells that co-expressed c-MAF and IL-17 (Figures 2C and 2D). On average, 50% of SI LP Th17 cells in SFB-colonized animals expressed c-MAF, which was similar to that of intestinal Foxp3⁺ Treg cells (Figures 2C and 2D). In contrast, compared to controls, other intestinal Th17 cells demonstrated either no change or decrease in the proportion of c-MAF⁺ cells (Figures 2C and 2D). The proportion of IL-10- and c-MAF-positive Th17 cells was not specifically increased in LI LP of SFB-positive animals (Figures S2A and S2D). SFB colonization generally did not increase the proportion of Foxp3⁻IL-17⁻IL-10⁺ (Tr1) cells, although slight increase was noted in the terminal ileum (Figure S2E). c-MAF induction in commensal Th17 cells preceded IL-10 expression and c-MAF expression was already elevated in IL-10^{GFP-} commensal Th17 cells (Figure 2E). However, c-MAF expression further increased in IL-10^{GFP+} SFB-induced Th17 cells (Figure 2F). Similarly to endogenous Th17 cells, naive SFB-specific 7B8 transgenic (Tg) CD4⁺ T cells adoptively transferred into SFB-positive wild-type (WT) C57BL/6 mice, differentiated into IL-10- and c-MAF-expressing Th17 cells (Figures 2G and 2H).

c-MAF is a transcription factor known to promote IL-10 expression in T cells and non-pathogenic Th17 cells.^{33,36} In

(B) Principal-component analysis (PCA) plot of RNA sequencing analysis of various intestinal LP Th17 cells. One experiment, n = 2–3 mice/group.

(C) Heatmap of core SFB Th17 cells program genes in bulk RNA-seq samples from (B). c-MAF controlled genes³⁶ are also marked on the right.

(D) Expression of selected cytokines and inhibitory receptors in LP Th17 cells in RNA-seq data from (B).

(E) Expression of selected transcription factors in LP Th17 cells in RNA-seq data from (B).

(F) Gene set enrichment analysis (GSEA) of genes elevated in SFB Th17 cells compared with genes elevated in exhausted CD4⁺ T cells.²⁶

(G) GSEA of genes elevated in SFB Th17 cells compared with genes elevated in mouse IL-10⁺ Th17 cells.¹²

(H) Expression of Tr1 signature genes in various intestinal LP Th17 cells.

(I) Venn diagram of leading-edge genes from GSEA of genes elevated in SFB Th17 cells and published datasets.^{12,13,29}

See also Figure S1.

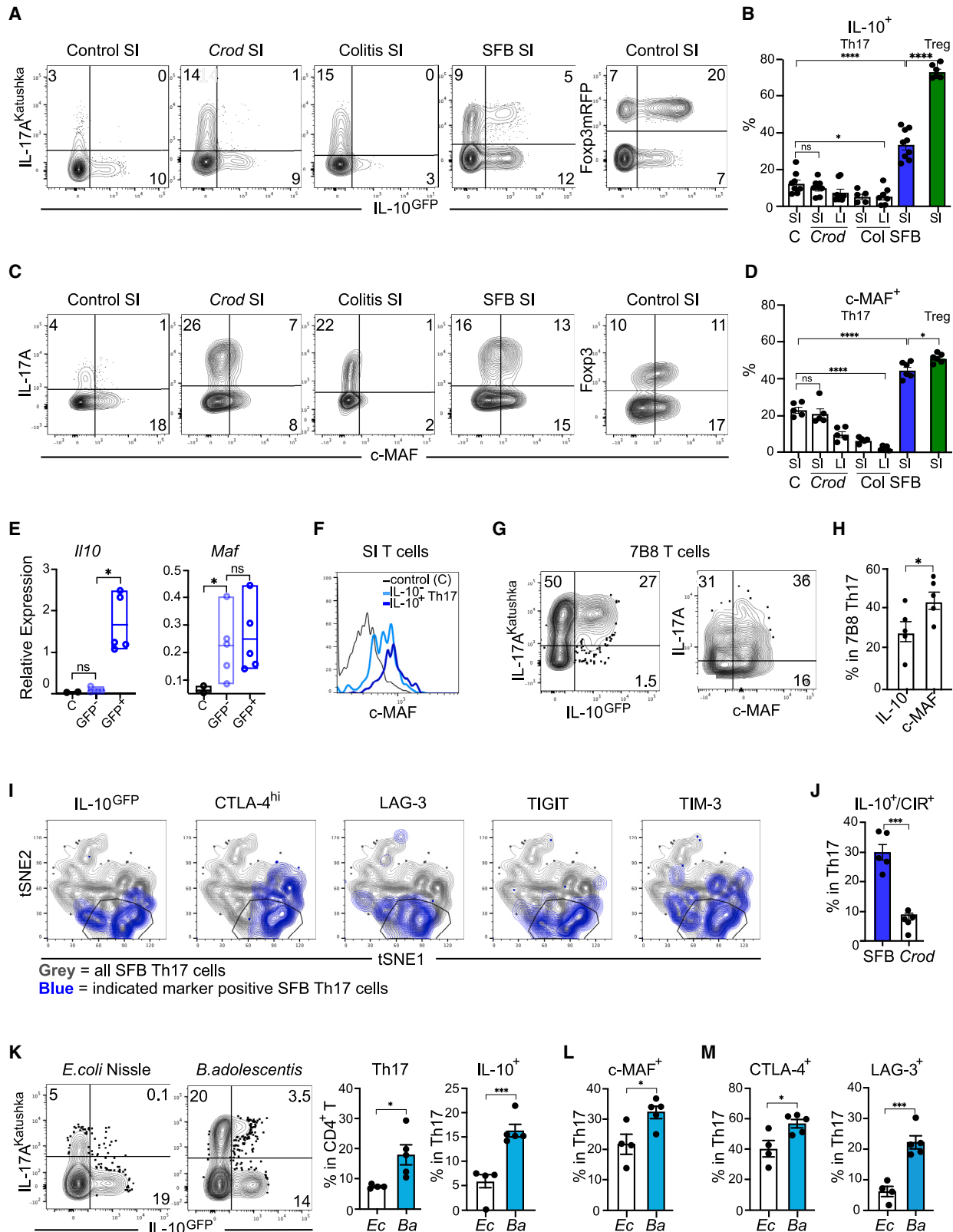


Figure 2. SFB Th17 cells express IL-10 and co-inhibitory receptors

(A and B) IL-10 expression in SI LP Th17 cells and Foxp3⁺ Treg cells from *Il10*^{GFP}/*Il17a*^{Katushka}/*Foxp3*^{mRFP} mice under various conditions. IL-17/IL-10 FACS plots in (A) gated on TCRβ⁺CD4⁺Foxp3^{mRFP}- lymphocytes. Foxp3/IL-10 FACS plot in (A) gated on TCRβ⁺CD4⁺IL-17^{Katushka}- lymphocytes.

(legend continued on next page)

addition, in several other T cell subsets, c-MAF imbues anti-inflammatory functions, even beyond IL-10.^{25,36} In particular, c-MAF controls an inhibitory gene module in CD4⁺ and CD8⁺ T cells that contains a number of co-inhibitory receptors, e.g., CTLA4, LAG3, TIM3, and TIGIT.²⁵ In agreement with a crucial role for c-MAF, SFB Th17 cells, but not other intestinal Th17 cells, contained a population that co-expressed IL-10 and co-inhibitory receptors (Figures 2I and 2J). Analysis of c-MAF target genes³⁶ in our RNA-seq datasets demonstrated that the core SFB Th17 cell signature was enriched in targets positively regulated by c-MAF (Figure 1C).

To investigate whether the induction of IL-10⁺ Th17 cells was restricted to SFB, we induced Th17 cells in *Il10^{GFP}/Il17a^{Katushka}/Foxp3^{mRFP}* reporter mice by oral gavage of *Bifidobacterium adolescentis*³⁷ (Figure S2F). Similar to SFB Th17 cells, *B. adolescentis*-induced SI LP Th17 cells expressed IL-10 and c-MAF, as well as the co-inhibitory receptors CTLA-4 and LAG-3 (Figures 2K–2M). Altogether our results suggest that c-MAF leads to expression of IL-10 and generally inhibitory T cell phenotype in commensal-specific SI LP Th17 cells.

The anti-inflammatory phenotype of SFB Th17 cells is driven by c-MAF

To directly assess the role of c-MAF in the acquisition of the Th17 cell regulatory phenotype we conditionally deleted c-MAF in Th17 cells by generating *Il10^{GFP}/Il17a^{Katushka}/Foxp3^{mRFP}/Il17a^{Cre}/Maf^{fllox/fllox}/R26^{STOP-YFP}* mice (*Maf^{ΔIL17}*). IL-17-expressing cells are also permanently labeled with YFP in these animals. We confirmed Th17 cell-specific deletion of c-MAF in SI LP Th17 cells of *Maf^{ΔIL17}* mice (Figure 3A). SFB Th17 cells were present in SI LP of *Maf^{ΔIL17}* mice, albeit at slightly decreased frequency compared with littermate controls (Figures 3B, S3A, and S3B). Other T cell and IL-17-expressing subsets were unchanged with exception of a decrease in IL-17⁺ γδ T cells (Figures S3C and S3D) as reported elsewhere.³⁸ c-MAF-deficiency in Foxp3⁺ Treg cells can also indirectly affect Th17 cell function through loss of IL-10 expression on Treg cells.³⁹ However, frequency and IL-10 production by Foxp3⁺ Treg cells were unaffected in *Maf^{ΔIL17}* mice (Figures 3C and S3C). In contrast, SFB Th17 cells lacked IL-10 expression in *Maf^{ΔIL17}* mice compared with littermate controls (Figures 3C,

3D, and S3E). Moreover, c-MAF-deficient SI LP Th17 cells also lost or decreased expression of other signature genes of the SFB anti-inflammatory program (Figures 3D and S3E). Instead, SI LP SFB Th17 cells from *Maf^{ΔIL17}* mice showed increased frequency of IFN-γ (Figure 3E) and increased expression of genes associated with inflammatory Th17 cells⁴⁰ (Figures 3D and S3E).

To examine changes in the overall transcriptional program, we performed single-cell RNA-seq (scRNA-seq) on purified YFP⁺ Th17 cells from SI LP of *Maf^{ΔIL17}* mice and littermate controls following SFB colonization. c-MAF-deficient SFB Th17 cells showed general loss of the SFB Th17 signature anti-inflammatory program (Figure 3F). In contrast to WT Th17 cells, the transcriptional program of SFB Th17 cells from *Maf^{ΔIL17}* mice resembled that of *Crod*-induced and colitogenic Th17 cells (Figure 3G), as well as that of published inflammatory EAE Th17 cells (Figure S3F). These results suggest that acquisition of an anti-inflammatory phenotype by commensal Th17 cells, including IL-10-expression, requires c-MAF.

Small-intestinal commensal Th17 cells have immunoregulatory functions

The foregoing results demonstrate that SFB Th17 cells express IL-10 and share transcriptional and phenotypic characteristics with IL-10-expressing immunoregulatory CD4⁺ T cells, such as Foxp3[−] Tr1 cells. We, therefore, investigated whether commensal Th17 cells can regulate the function of other CD4⁺ T cells. To evaluate inhibitory effects on T cell proliferation, we first compared the proliferation of responder CD4⁺ T cells *in vitro* in the presence or absence of purified intestinal Th17 cells. *Citrobacter*-induced Th17 cells from SI or LI did not affect proliferation of responder T cells (Figure 4A). In contrast, co-culture with SFB-induced SI LP Th17 cells led to inhibition of responder T cell proliferation (Figure 4A). Inhibition of proliferation did not correlate with preferential expansion of intestinal Th17 cells in these assays, because SFB Th17 cells demonstrated lower proliferative capacity than *Citrobacter* Th17 cells (Figure 4B). Inhibition of proliferation by SFB Th17 cells required IL-10 signaling because addition of IL-10R-blocking antibody to the co-cultures rescued responder cell proliferation (Figure 4C). Moreover, SFB Th17 cells did not inhibit proliferation of responder CD4⁺ T cells that lacked expression of IL-10R

(B) Frequency of IL-10^{GFP+} Th17 (TCRβ⁺CD4⁺Foxp3^{mRFP−}IL-17^{Katushka+}) or Treg (TCRβ⁺CD4⁺Foxp3^{mRFP+}) cells. Three independent experiments, n = 5–9 mice/group.

(C and D) c-MAF expression (intracellular staining) in SI LP Th17 cells and Foxp3⁺ Treg cells. FACS plots in (C) gated on TCRβ⁺CD4⁺ LP lymphocytes.

(D) Frequency of c-MAF⁺ Th17 (TCRβ⁺CD4⁺IL-17[−]) or Treg (TCRβ⁺CD4⁺Foxp3⁺) cells. Two independent experiments, n = 5–6 mice/group.

(E) qPCR for *Il10* and *Maf* transcripts in IL-10^{GFP−} and IL-10^{GFP+} SFB Th17 cells (TCRβ⁺CD4⁺Foxp3^{mRFP−}IL-17^{Katushka−}) and IL-10^{GFP−}/IL-17^{Katushka−}/Foxp3^{mRFP−} control (C) CD4⁺ SI LP T cells. Two independent experiments, n = 2–5 mice/group.

(F) Representative histograms of c-MAF expression (intracellular staining) in IL-10^{GFP−} and IL-10^{GFP+} Th17 cells and control CD4⁺ T cells from SI LP of SFB-colonized *Il10^{GFP}/Il17a^{Katushka}/Foxp3^{mRFP}* mice. Two independent experiments, n = 2–5 mice/group.

(G and H) Naive SFB-specific 7B8 TCR Tg CD4⁺ T cells from 7B8 triple reporter mice were adoptively transferred into SFB-colonized congenic wild-type mice. IL-10 (GFP) and c-MAF (intracellular staining) in transferred CD4⁺ T cells was examined 1 week later. FACS plots gated on Ly5.1⁺CD4⁺TCRβ⁺Foxp3[−] transferred 7B8 cells. Bar plots further gated on IL-17⁺ Th17 cells. Two independent experiments, n = 5 mice/group.

(I and J) t-distributed stochastic neighbor embedding (tSNE) analysis based on multi-parameter flow cytometry of IL-10 and co-inhibitory receptors (CIR) expression in LP Th17 cells from SFB-colonized (I and J) or *Citrobacter rodentium* (*Crod*) infected (J) *Il10^{GFP}/Il17a^{Katushka}/Foxp3^{mRFP}* mice. Plots gated on Ly5.1⁺CD4⁺TCRβ⁺Foxp3^{mRFP−}IL-17^{Katushka+} cells. Two independent experiments, n = 5 mice/group.

(K) Induction of Th17 cells and IL-10⁺ Th17 cells in SI LP of *Il10^{GFP}/Il17a^{Katushka}/Foxp3^{mRFP}* mice after oral gavage of *E. coli* (*Ec*) or *B. adolescentis* (*Ba*) every other day for 2 weeks. IL-17/IL-10 FACS plots gated on TCRβ⁺CD4⁺Foxp3^{mRFP−} lymphocytes. Two independent experiments, n = 4–5 mice/group.

(L and M) Frequency of c-MAF⁺ (L), LAG-3⁺ and CTLA-4⁺ (M) SI LP Th17 cells in the experiments in (K). Two independent experiments, n = 4–5 mice/group. See also Figure S2.

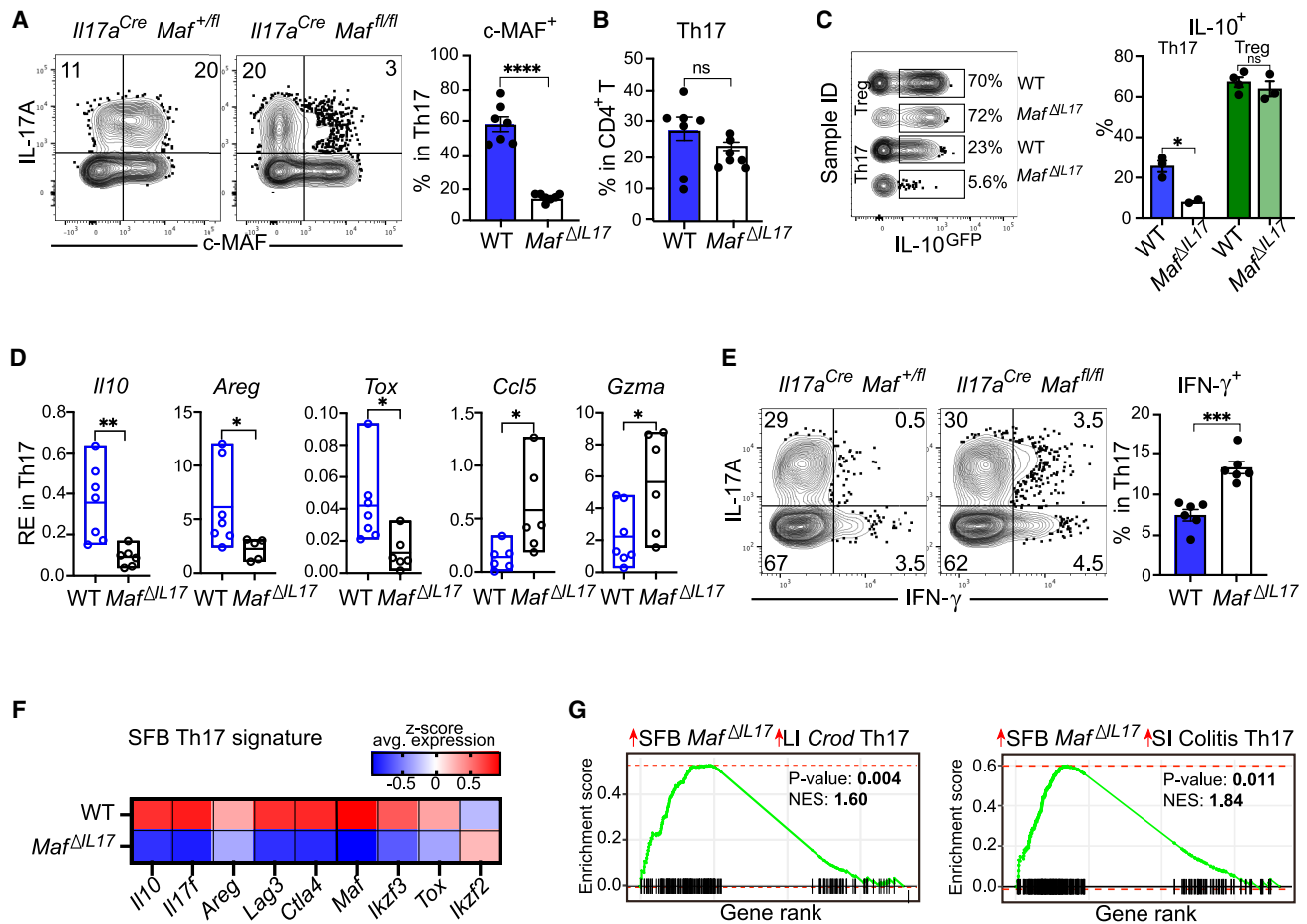


Figure 3. c-MAF drives anti-inflammatory identity of intestinal commensal Th17 cells

(A) Intracellular staining for c-MAF in CD4⁺ T cells and Th17 cells from SI LP of *Il17a^{Cre}/Maf^{ΔIL17}* (*Maf^{ΔIL17}*) mice and *Il17a^{Cre}/Maf^{fl/fl}* (WT) littermates. Three independent experiments, n = 5–7 mice/group.

(B) Frequency of Th17 cells (intracellular staining) in SI LP of WT and *Maf^{ΔIL17}* mice. Three independent experiments, n = 7 mice/group.

(C) Frequency of IL-10^{GFP+} SI LP Th17 cells and Foxp3⁺ Treg cells from *Il10^{GFP}/Il17a^{Katushka}/Foxp3^{mRFP}/R26^{STOP-YFP}/Il17a^{Cre}/Maf^{ΔIL17}* (*Maf^{ΔIL17}*) and littermate control (WT) mice. Plots gated on TCR β ⁺CD4⁺Foxp3^{mRFP}-IL-17^{Katushka}⁺ (Th17) or TCR β ⁺CD4⁺Foxp3^{mRFP}⁺ (Treg) lymphocytes. Two independent experiments, n = 2–4 mice/group.

(D) Quantitative PCR of *Il10*, *Areg*, *Tox*, *Ccl5*, and *Gzma* mRNA in FACS-purified SI LP Th17 cells (TCR β ⁺CD4⁺Foxp3^{mRFP}-IL-17^{Katushka}⁺) from WT and *Maf^{ΔIL17}* mice. Two independent experiments, n = 6–7 mice/group.

(E) Intracellular staining for IL-17 and IFN- γ in (left) CD4⁺ T (TCR β ⁺CD4⁺) and (right) Th17 (TCR β ⁺CD4⁺IL-17⁺) cells from SI LP of WT and *Maf^{ΔIL17}* mice. Two independent experiments, n = 6 mice/group.

(F) Heatmap of selected SFB Th17 cell signature genes in scRNA-seq of FACS-purified SI LP Th17 cells (TCR β ⁺CD4⁺Foxp3^{mRFP}-IL-17^{YFP}⁺) from WT and *Maf^{ΔIL17}* (*Foxp3^{mRFP}/R26^{STOP-YFP}/Il17a^{Cre}/Maf^{ΔIL17}*) mice. One experiment, n = 2–3 mice/group.

(G) GSEA of top 200 elevated genes in *Maf^{ΔIL17}* SI LP SFB Th17 cells (TCR β ⁺CD4⁺Foxp3^{mRFP}-IL-17^{YFP}⁺) compared with genes elevated in LI *Crod* Th17 cells and SI colitis Th17 cells in bulk RNA-seq datasets in Figure 1.

See also Figure S3.

(Figure 4D). SFB Th17 cells also express co-inhibitory receptors (Figures 2I and 2J). Blocking antibodies against CTLA-4, but not LAG-3, partially reduced the inhibitory ability of SI LP SFB Th17 cells (Figures 4E and 4F). In addition, c-MAF-deficient SI LP SFB Th17 cells lost the ability to suppress responder T cell proliferation (Figure 4G). These results suggest that intestinal commensal Th17 cells can exert regulatory functions *in vitro* in an IL-10 and c-MAF-dependent manner.

To evaluate immunoregulatory functions of SFB Th17 cells *in vivo*, we considered their localization. SFB Th17 cells are exclusively present in SI LP.^{6,41–43} Compared with other Th17

cells in our dataset, SFB Th17 cells express several chemokine receptors associated with tissue residency or homing to SI, e.g., *Ccr9*, *Ccr5*, and *Ccr1*, (Figure S4A).^{44–46} In addition, SFB Th17 cells almost uniformly express the tissue retention factor CD69 (Figure S4B).⁴⁷ Purified small-intestinal SFB Th17 cells homed exclusively to the SI LP, but not to other tissues, including other intestinal tissues (Figure S4C). Thus, SFB Th17 cells possess features of tissue-resident CD4⁺ T cells. We, therefore, investigated whether SFB Th17 cells exert immunoregulatory functions locally in the SI. Adoptive transfer of purified intestinal SFB Th17 cells into RAG1-deficient animals (Figure 4H) inhibited

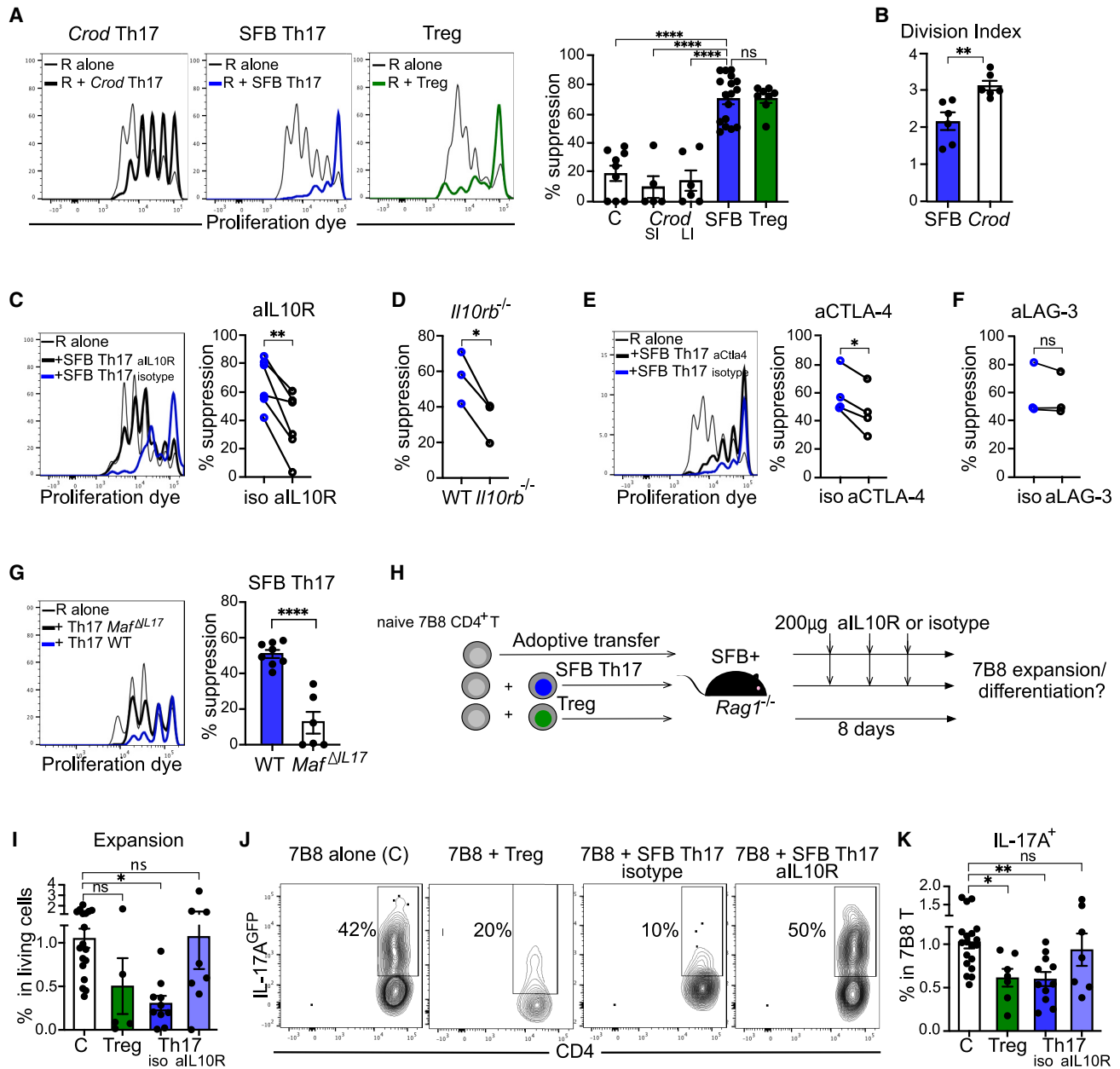


Figure 4. Regulatory functions of commensal Th17 cells

(A) *In vitro* suppression assay. FACS-purified intestinal LP Th17 cells (TCRβ⁺CD4⁺Foxp3^{mRFP}-IL-17^{GFP+}) from SFB-colonized or *Citrobacter rodentium*-infected (*Crod*) mice or SI LP Treg cells (TCRβ⁺CD4⁺Foxp3^{mRFP+}) were co-cultured with WT naive responder CD4⁺ T cells from spleen of untreated mice as described in STAR Methods. (Left) Proliferation of CTV-stained responder T cells (R) on day 4. (Right) Percent suppression calculated as described in STAR Methods. Cumulative of four independent experiments, n = 2–3 technical replicates/experiment. Each dot represents a technical replicate.

(B) Division index (see STAR Methods) of CTV-labeled SFB and *Crod* LP Th17 cells in *in vitro* suppression assay. One experiment, n = 3 mice/group and 2 technical replicates/mouse. Each dot represents a technical replicate.

(C) Proliferation of WT responder CD4⁺ T cells (R) alone or co-cultured with FACS-purified SI LP SFB Th17 cells (TCRβ⁺CD4⁺Foxp3^{mRFP}-IL-17^{GFP+}) in the presence of blocking anti-IL-10R antibody or isotype control. Five independent experiments, n = 2–3 technical replicates/experiment. Significance, paired t test.

(D) Inhibition of proliferation of WT or *Il10rb*^{-/-} responder CD4⁺ T cells by purified WT SI LP SFB Th17 cells (TCRβ⁺CD4⁺Foxp3^{mRFP}-IL-17^{GFP+}). Three independent experiments, n = 2–3 technical replicates/experiment. Significance, paired t test.

(E) Proliferation of WT responder CD4⁺ T cells (R) alone or co-cultured with FACS-purified SI LP SFB Th17 cells (TCRβ⁺CD4⁺Foxp3^{mRFP}-IL-17^{GFP+}) in the presence of blocking anti-CTLA-4 antibody or isotype control. Four independent experiments, n = 2–3 technical replicates/experiment. Significance, paired t test.

(F) Proliferation of WT responder CD4⁺ T cells (R) alone or co-cultured with FACS-purified SI LP SFB Th17 cells (TCRβ⁺CD4⁺Foxp3^{mRFP}-IL-17^{GFP+}) in the presence of blocking anti-LAG3 antibody or isotype control. Three independent experiments, 2–3 technical replicates/experiment. Significance, paired t test.

(legend continued on next page)

expansion (Figure 4I) and IL-17 production (Figures 4J and 4K) of co-transferred naive 7B8 Tg CD4⁺ T cells. The inhibition was similar to that exerted by SI LP Foxp3⁺ Treg cells (Figures 4I–4K). Moreover, this inhibition occurred only in the SI LP and was not observed in mesenteric lymph nodes (mLN) (Figure S4D). Neutralization of IL-10-signaling *in vivo*, reduced commensal Th17-cell-mediated inhibition of CD4⁺ T cell expansion and cytokine production in SI LP (Figures 4I–4K). The foregoing results suggest that commensal Th17 cells can exert immunoregulatory functions and curb effector T cell activity both *in vitro* and *in vivo* in an IL-10-dependent manner.

Commensal Th17 cells are heterogeneous and contain a progenitor TCF1⁺ subset

To further examine the heterogeneity of commensal Th17 cells, we purified Th17 cells from SI LP of SFB-colonized *Il17a*^{Katushka}/*Foxp3*^{mRFP} reporter mice and performed scRNA-seq. Uniform manifold approximation and projection for dimensional reduction (UMAP) analysis of 5,721 recovered single SI LP Th17 cells showed several transcriptionally distinct clusters (Figure 5A). We annotated these clusters into functional sets based on the genes that were differentially expressed relative to all other clusters (Figures 5B and 5C). Apart from two small clusters enriched in proliferation and interferon stimulated genes (ISGs), respectively, the majority (97%) of intestinal Th17 cells had terminally differentiated or progenitor/stem-like phenotypes (Figures 5B and 5C). Terminally differentiated Th17 cells belonged to two distinct types with either activated (C1 and C3) or inhibitory (C2 and C6) phenotype (Figures 5B and 5C). Activated Th17 cells expressed genes associated with T cell activation and intestinal tissue residency, e.g., *Cd69*, *Cd28*, *Jun*, *Ccr9*, *Ccr2*, *Ccr5*, and *Ccl20*. In contrast, Th17 cells with inhibitory phenotype expressed inhibitory and tissue-repair genes, e.g., *Lag3*, *Havcr2* (*Tim3*), *IL17f*, *Tgfb1*, and *Areg* (Figure 5B). Cells in C1 and C6 contained higher expression of the corresponding effector programs (Figure 5B). Both types of terminally differentiated Th17 cells expressed *Il10* (Figure 5D).

Pathway analysis of DEGs between the two effector groups demonstrated differences not only in activation, but also in their metabolic profile (Figure 5E). Metabolism is an established regulator of T cell functionality. We, therefore, applied the COMPASS algorithm⁴⁸ to compare metabolic states of the two most divergent IL-10-expressing clusters (C1 and C6). COMPASS predicted that cells in C1 had increased levels of glycolysis and those in C6 had increased fatty acid oxidation and amino acid metabolism (Figure 5F). These differences parallel those previously described between pathogenic Th17 cells vs non-pathogenic Th17 cells and Foxp3⁺ Treg cells.⁴⁸

c-MAF targets were specifically enriched in both inhibitory and activated IL-10⁺ Th17 cells (Figure 5G). We next examined the role

of c-MAF by purifying YFP⁺ SI LP Th17 cells from *Maf*^{ΔIL-17} mice and WT littermate controls and performing scRNA-seq. Analysis of more than 10,000 SI LP Th17 cells identified similar UMAP functional clustering (Figures S5A and S5B). Further analysis revealed that both types of IL-10⁺ Th17 cell groups required c-MAF for IL-10 expression (Figure 5H). Th17-specific deletion of c-MAF led to a decrease in the most differentiated IL-10⁺ Th17 cell clusters (Figures 5I and 5J). In addition, Th17-specific deletion of c-MAF resulted in loss of the overall anti-inflammatory program of both activated and inhibitory effector IL-17⁺ Th17 cells (Figures 5K and S5C). In addition, conditional deletion of c-MAF resulted in an increase in the proportion of YFP⁺IL-17⁻ (ex-Th17) cells with an inflammatory phenotype (Figures 5I–5L and S5D). Thus, c-MAF not only drives the anti-inflammatory SFB Th17 cell program but also inhibits conversion into inflammatory ex-Th17 cells.

Progenitor-like commensal Th17 cells (clusters C4, C5, and C7 on Figure 5A) were defined by expression of stem-like features, e.g., *Tcf7*, *Il7r*, and *Slamf6*^{49,50} (Figures 5A, 6A, and S6A). We confirmed co-expression of TCF1 and IL-7R on a subset of commensal SI LP Th17 cells by flow cytometry (Figure 6B). In agreement with the scRNA-seq data, TCF1 expression decreased in IL-10⁺ SFB Th17 cells (Figure 6C). In contrast, a subset of TCF1⁺ SFB Th17 cells expressed low levels of c-MAF (Figure 6D). Progenitor-like SI LP Th17 cells had decreased ability to suppress T cell proliferation *in vitro*, compared with TCF1⁻IL-10⁺ Th17 cells (Figures 6E, S6B, and S6C). Trajectory analysis of scRNA-seq data from SI LP Th17 cells revealed three distinct trajectories for progenitor-like TCF1⁺ Th17 cells in cluster C4 leading to each of the two effector IL-10⁺ populations and to the progenitor-like group (Figure 6F). This suggests that TCF1⁺ Th17 cells have the potential to self-renew and to generate TCF1⁻IL-10⁺ Th17 cells. We also identified a similar TCF1⁺ Th17 cell subset in the LI LP of animals infected with *Crod* (Figures S6D and S6E). To confirm experimentally the progenitor nature of TCF1⁺ Th17 cells, we generated *Tcf7*^{mCherry} reporter mice and crossed them to *Il17a*^{GFP} and *Il10*^{Venus} reporter animals (Figures S6F and S6G). Analysis of SI LP Th17 cells confirmed that TCF1^{mCherry+} Th17 cells do not express IL-10 (Figures 6G and 6H). Next, we purified TCF1^{mCherry+} Th17 cells from SI LP of SFB-positive animals and adoptively transferred these cells into SFB-colonized WT mice. TCF1^{mCherry+} Th17 cells homed to SI LP immediately after transfer and gave rise to TCF1⁻ Th17 cells at later timepoints (Figure 6I). Purified SFB TCF1⁺ LP Th17 cells also differentiated into TCF1⁻IL-10⁺ Th17 cells upon T cell receptor (TCR) stimulation *in vitro*, in contrast to TCF1⁺ LP Th17 cells from *Crod*-infected mice (Figure 6J). In these experiments, we could not recover enough cells following adoptive transfer or *in vitro* culture of TCF1⁻ Th17 cells, suggesting that they lose the ability to self-renew and to propagate an

(G) Proliferation of WT responder CD4⁺ T cells (R) alone or co-cultured with SI LP SFB Th17 cells (TCRβ⁺CD4⁺Foxp3^{mRFP}-IL-17^{YFP+}) from WT or *Maf*^{ΔIL-17} mice. Cumulative of three independent experiments, n = 2–3 technical replicates/experiment. Each datapoint represents a technical replicate.

(H) Experimental schematic of *in vivo* suppression assay.

(I–K) Expansion/frequency (I) and cytokine (IL-17) production (J and K) of naive 7B8 CD4⁺ T cells (Ly5.1⁺) in SI LP 8 days after transfer into SFB-colonized RAG1-deficient mice alone (C) or with co-transfer of SI LP Treg cells (TCRβ⁺CD4⁺Foxp3^{mRFP+}) or SI LP SFB Th17 cells (TCRβ⁺CD4⁺IL-17^{GFP+}) with and without neutralization of IL-10 signaling by intraperitoneal injection of an anti-IL-10R or isotype control antibody. Plots gated on Ly5.1⁺TCRβ⁺CD4⁺ (7B8) SI LP lymphocytes. (I and K) Data were normalized to the average of the corresponding control group. Cumulative of six independent experiments, n = 7–17 mice/group. See also Figure S4.

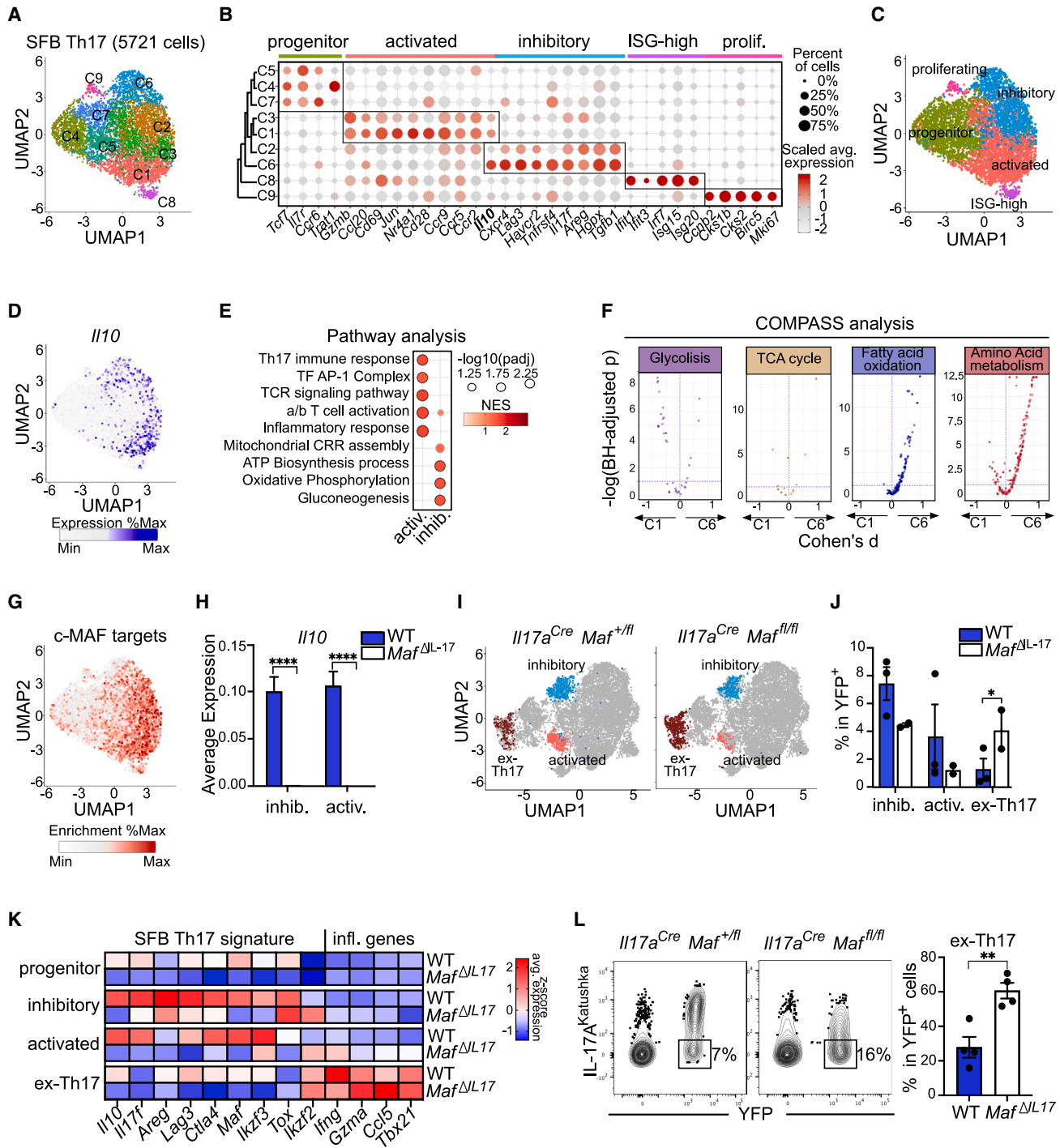


Figure 5. Commensal Th17 cells are heterogeneous and contain two IL-10⁺ populations

(A) UMAP clustering following scRNA sequencing of 5,721 SFB SI LP Th17 cells (TCRβ⁺CD4⁺Foxp3^{mRFP}-IL-17^{Katushka}) sorted from *I110^{GFP}/I117a^{Katushka}/Foxp3^{mRFP}* reporter mice.

(B) Functional grouping of SI LP Th17 cell clusters in (A) based on expression of select marker genes.

(C) UMAP with annotation of the functional groups in (B).

(D) Expression of *I110* in individual SFB SI LP Th17 cells in the UMAP clustering in (A).

(E) Pathway analysis of differentially expressed genes between activated and inhibitory IL-10⁺ expressing groups.

(F) COMPASS analysis for metabolic pathways in the two most differentiated IL-10⁺ UMAP clusters, C1 and C6.

(G) GSEA for c-MAF target genes³⁶ in individual SFB SI LP Th17 cells in the UMAP clustering in (A).

(legend continued on next page)

immune response (data not shown). Altogether our results suggest that IL-10⁺ commensal Th17 cells in the SI LP are heterogeneous and differentiate from TCF1⁺ progenitor Th17 cells following increase in c-MAF and decrease in TCF1 expression.

To further examine the phenotype of TCF1⁺ progenitor Th17 cells, we performed bulk RNA-seq of purified TCF1⁺ and TCF1⁻ intestinal Th17 cells from SI LP of SFB-colonized and LI LP of *Crod*-infected *Tcf7^{mCherry}/Il17a^{GFP}* reporter mice. SFB TCF1⁺ Th17 progenitors differed from *Crod* Th17 progenitors (Figures 6K and 6L). Gene set enrichment analysis showed that SFB TCF1⁺ progenitors were enriched in the core SFB anti-inflammatory signature compared with *Crod* TCF1⁺ progenitors, which resembled the general *Crod* Th17 program (Figure 6M). For both types of microbes, the transcriptional program of progenitor Th17 cells most closely resembled that of the corresponding TCF1⁻ Th17 cells (Figure 6K) with TCF1⁺ and TCF1⁻ SFB Th17 cells overlapping most closely and expressing the least number of DEGs (Figures 6K and 6L). SFB Th17 cell signature anti-inflammatory genes were enriched in SFB TCF1⁺ Th17 cells compared with *Crod* TCF1⁺ Th17 cells and, vice versa, inflammatory signature genes were enriched in *Crod* TCF1⁺ Th17 cells (Figures 6M, 6N, and S6H). *Maf*, *Tox*, and other genes associated with the SFB Th17 program were already elevated in TCF1⁺ SFB progenitors and further increased in TCF⁻ SFB effectors (Figures 6N, 6O, S6H, and S6I).

We next investigated whether inflammatory cytokines could affect the transcriptional program of commensal Th17 progenitors. *In vitro* stimulation of purified SI LP TCF1⁺IL-17⁺IL-10⁻ Th17 cells in the presence of IL-1 β and IL-23 resulted in decrease in their ability to differentiate into IL-10⁺ effector Th17 cells (Figure 6P) and instead induced production of IFN- γ (Figure 6Q). Combined our results suggest that LP TCF1⁺ progenitor commensal Th17 cells are transcriptionally poised to differentiate to anti-inflammatory effectors but retain the ability to respond to inflammatory queues from the environment.

IL-10 signaling and iM ϕ in terminal ileum instruct acquisition of Th17 anti-inflammatory phenotype

We next investigated the signals and participating innate immune cells that facilitate the differentiation of TCF1⁺ progenitors into IL-10-expressing anti-inflammatory Th17 cells. TCF1⁺ progenitor Th17 cells were present exclusively in the SI LP and not in mLN and adoptively transferred TCF1⁺ progenitor Th17 cells homed exclusively to the SI LP (Figure S7A). In addition, although TCF1⁺ Th17 cells were present in both duodenum and ileum, TCF1⁻IL-10⁺ Th17 cells were specifically present in the terminal ileum (Figures 7A and 7B). Purified ileal TCF1⁺

SFB Th17 cells had an increased capacity to generate TCF1⁻IL-10⁺ Th17 cells *in vitro*, compared with TCF1⁺ SFB Th17 cells from duodenum or SI LP TCF1⁺ Th17 cells from *Citrobacter*-infected mice (Figure S7B). These results suggest that commensal precursor Th17 cells acquire IL-10 expression locally in the terminal ileum under the guidance of signals from the gut microenvironment.

IL-10 induces Tr1 cell differentiation *in vitro*⁵¹ and is required for the maintenance of IL-10 expression in Tr1 cells and Foxp3⁺ Treg cells.^{52,53} We, therefore, investigated the role of IL-10 in generation of IL-10-producing SFB Th17 cells. For this, we crossed *Il10^{GFP}/Il17a^{Katushka}/Foxp3^{mRFP}* reporter mice to SFB-specific 7B8 TCR Tg mice on a Ly5.1 congenic background. We then adoptively transferred naive 7B8.Ly5.1 triple reporter CD4⁺ T cells into WT and IL-10-deficient animals and examined SFB-specific Th17 cell induction, as well as the phenotype of the induced Th17 cells (Figure 7C). 7B8 CD4⁺ T cells differentiated into IL-10-expressing Th17 cells in SI LP of WT control animals (Figure 7D). In contrast, although WT 7B8 CD4⁺ T cells decreased TCF1 expression and became Th17 cells in *Il10^{-/-}* mice, they had decreased proportion of IL-10⁺ Th17 cells (Figures 7D, S7C, and S7D). Moreover, 7B8 CD4⁺ Th17 cells had decreased expression of c-MAF in the absence of environmental IL-10 (Figure 7E). Therefore, IL-10 is required for the induction of c-MAF and IL-10 in commensal Th17 cells. To investigate the source of IL-10, we next transferred triple reporter 7B8 Tg CD4⁺ T cells into recipients with conditional deletion of IL-10 in T cells (*Cd4^{Cre}/Il10^{fllox/fllox}* or *Il10^{dT}* mice). Despite similar Th17 cell differentiation, 7B8 Th17 cells had decreased c-MAF and IL-10 expression in the absence of IL-10 production by T cells (Figures 7F, 7G, and S7E). These results suggest that IL-10 production by CD4⁺ T cells is required for induction of IL-10 expression by commensal Th17 cells.

To investigate whether IL-10 acts directly on the differentiating commensal Th17 cells, we transferred control and *Il10rb^{-/-}* triple reporter CD4⁺ T cells into WT recipients (Figure 7H). IL-10R β -deficient CD4⁺ T cells differentiated into Th17 cells similarly to controls (Figure S7F) and contained similar proportion of c-MAF⁺ and IL-10⁺ Th17 cells (Figures 7I and S7G). In contrast, despite unimpeded Th17 cell differentiation, WT SFB-specific CD4⁺ T cells did not become IL-10⁺ or c-MAF⁺ Th17 cells when transferred into IL-10R β -deficient recipients (Figures 7J, 7K, and S7H). Combined, these results suggest that IL-10 does not directly act on differentiating commensal Th17 cells.

We previously reported that iM ϕ participate in the induction of SFB-specific Th17 cells.⁵⁴ Moreover, IL-10R β signaling in iM ϕ is crucial for establishment of intestinal homeostasis.⁵⁵

(H) Expression of *Il10* mRNA in indicated functional groups in SI LP SFB Th17 cells from WT (*Foxp3^{mRFP}/R26^{STOP-YFP}/Il17a^{Cre}/Maf^{fllox/+}*) and *Maf^{dIL17}* (*Foxp3^{mRFP}/R26^{STOP-YFP}/Il17a^{Cre}/Maf^{fllox/fllox}*) mice, based on scRNA-seq of SI LP Th17 cells sorted based on YFP expression. Based on the functional clustering in Figure S5B. SI LP SFB Th17 cells from individual mice were identified by hash-tagging of scRNA-seq samples. n = 2–3 mice/group.

(I) Frequency of cells in clusters C7 (ex-Th17), C8 (inhibitory), and C10 (activated) based on the UMAP clustering in Figure S5A. Data from hash-tagged scRNA-seq samples from WT and *Maf^{dIL17}* (*Foxp3^{mRFP}/R26^{STOP-YFP}/Il17a^{Cre}/Maf^{fllox/fllox}*) mice. Data integrated from n = 2–3 mice/group.

(J) Frequency of cells in the clusters in (I). Data points represent individual mice.

(K) Heatmap of Z score of average expression of selected SFB Th17 signature genes and inflammatory genes in indicated functional groups from WT and *Maf^{dIL17}* mice based on UMAP in Figure S5B.

(L) (Left) IL-17^{Katushka} and ROSA^{YFP} expression in SI LP CD4⁺ T cells (TCR β ⁺CD4⁺Foxp3^{mRFP}-) from SI LP of WT and *Maf^{dIL17}* mice. (Right) Frequency of ex-Th17 cells (TCR β ⁺CD4⁺IL-17^{YFP}IL-17^{Katushka}-) within YFP⁺ cells. n = 4 mice/group. See also Figure S5.

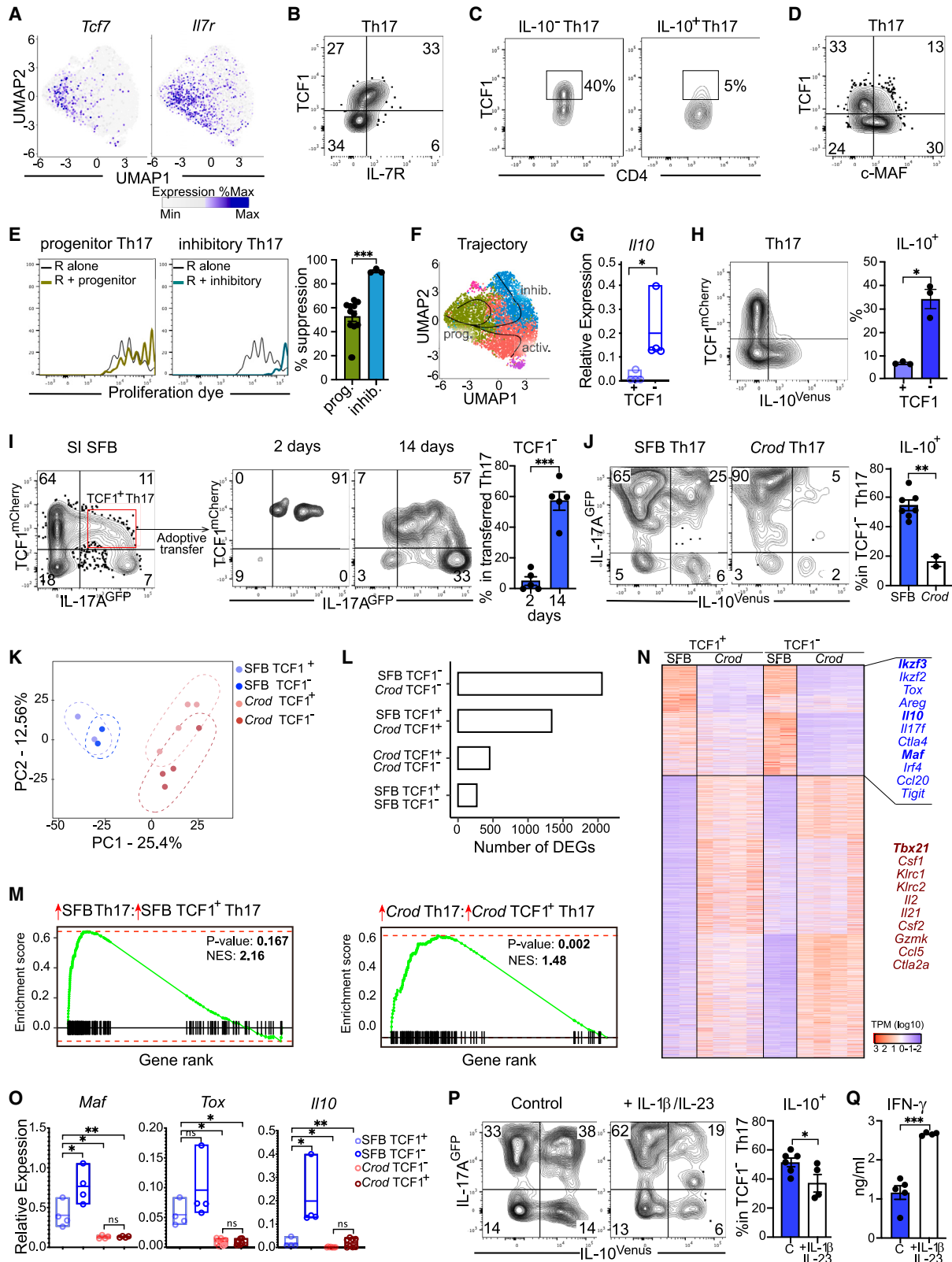


Figure 6. Commensal Th17 cells contain a progenitor TCF1⁺ population

(A) Expression of *Tcf7* and *Il7r* mRNA in individual SFB SI LP Th17 cells in the UMAP clustering in Figure 5A.

(B) TCF1 and IL-7R expression in SI LP SFB Th17 cells. Gated on TCRβ⁺CD4⁺IL-17⁺ lymphocytes.

(legend continued on next page)

We, therefore, investigated whether IL-10R β signaling in iM ϕ is required for induction of IL-10 expression by SFB Th17 cells. To conditionally delete IL-10R β in iM ϕ , we generated mixed bone marrow (BM) chimeras in which lethally irradiated WT mice were reconstituted with a 1:1 BM mixture from *Ccr2*^{DTR} and *Il10rb*^{-/-} animals (Figure 7L). We previously showed that diphtheria toxin (DT) injection leads to specific loss of iM ϕ , but not intestinal dendritic cells in *Ccr2*^{DTR} animals.⁵⁴ Administration of DT in the mixed chimeras leads to deletion of *Ccr2*^{DTR} iM ϕ , but not *Il10rb*^{-/-} iM ϕ , resulting in an iM ϕ population that specifically lacks IL-10R β expression (Figure S7I). SFB-specific CD4⁺ T cells differentiated into IL-10⁺ Th17 cells when transferred into DT-treated control *Ccr2*^{DTR}:WT BM chimeras (Figure 7M). In contrast, although 7B8 CD4⁺ T cells differentiated similarly to Th17 cells in recipients with conditional deletion of IL-10R β in iM ϕ (Figure S7J), these Th17 cells had decreased IL-10 and c-MAF expression (Figures 7M and 7N). Altogether the foregoing results suggest that iM ϕ detect T cell-derived IL-10 to induce or maintain production of IL-10 by commensal Th17 cells.

DISCUSSION

Th17 cells are defined by the expression of the signature cytokine IL-17A. Although Th17 cells were originally described as pro-inflammatory, it is now appreciated that there is a considerable range in Th17 cell functionality.^{12,13,15,22,48,49} Homeostatic non-pathogenic Th17 cells have been described, but their functions are ill-defined. In the gut, the role of commensal-induced Th17 cells is unclear. Although absence of SFB Th17 cells leads to slight SFB increase in the gut lumen,¹⁰ control of SFB is mainly mediated by type 3 innate lymphoid cells.⁵⁶ SFB Th17 cells were originally considered pro-inflammatory. However, it was later

shown that SFB Th17 cells possess a non-pathogenic transcriptional program.²⁴ Our results demonstrate that SFB Th17 cells have a regulatory anti-inflammatory program and can produce IL-10. We further found that *Bifidobacterium adolescentis* induces Th17 cells with a similar phenotype, which suggests that IL-10 production by Th17 cells is characteristic of multiple commensal species. Thus, commensal Th17 cells may also play role in maintaining mucosal homeostasis. Indeed, intestinal SFB Th17 cells prevent metabolic disease in the context of diet-induced obesity.⁵⁷ In addition, herein we report that SFB Th17 cells suppress intestinal effector T cell responses via IL-10.

In contexts of intestinal inflammation, LP IL-10⁺ Th17 cells transdifferentiate to Tr1 cells.²² SFB-induced IL-10⁺ Th17 cells in our study also express Tr1-associated genes. However, using scRNA-seq of YFP⁺ CD4⁺ T cells from *Il17a*^{Cre}/*R26*^{STOP-YFP} mice we found few YFP⁺ CD4⁺ T cells without IL-17 transcripts (ex-Th17 cells) in WT animals, and therefore little evidence for trans-differentiation of SFB Th17 cells at steady state. This is also in agreement with a prior study that concluded that SI LP SFB Th17 cells possess little plasticity.²⁴ In contrast, after Th17-specific ablation of c-MAF, we found a considerable population of ex-Th17 cells, which expressed pro-inflammatory genes. Therefore, c-MAF not only maintains IL-10 expression in commensal Th17 cells but also prevents trans-differentiation into pro-inflammatory CD4⁺ T cells. Whether commensal Th17 cells can become fully functional Tr1 cells remains to be investigated.

In our study, SFB Th17 cells inhibited expansion and cytokine production of effector CD4⁺ T cells in an IL-10 and c-MAF-dependent manner. However, they also expressed several inhibitory receptors. Indeed, in our hands, blockade of CTLA-4, but not LAG-3, also partially inhibited suppression in *in vitro* assays.

- (C) Intracellular staining for TCF1 in purified IL-10^{GFP-} and IL-10^{GFP+} SI LP SFB Th17 cells (TCR β ⁺CD4⁺Foxp3^{mRFP-}IL-17^{Katushka+}).
- (D) Intracellular staining for TCF1 and c-MAF in SI LP SFB Th17 cells. Gated on TCR β ⁺CD4⁺IL-17⁻ lymphocytes.
- (E) FACS-purified SI LP SFB progenitor Th17 cells (TCR β ⁺CD4⁺Foxp3^{mRFP-}IL-17^{Katushka+}IL-10^{GFP-}IL-7R⁺) and SI LP SFB inhibitory Th17 cells (TCR β ⁺CD4⁺Foxp3^{mRFP-}IL-17^{Katushka+}IL-10^{GFP+}LAG-3⁺) were co-cultured with WT naive responder CD4⁺ T cells. (Left) Proliferation of CTV-stained responder T cells (R) on day 4. (Right) Percent suppression. Cumulative of three independent experiments. Each dot represents a technical replicate.
- (F) Trajectory analysis of scRNA-seq data in Figure 5A with a start node in C4. UMAP annotation as in Figure 5C.
- (G) Quantitative PCR for *Il10* mRNA in FACS-purified TCF1^{mCherry+} and TCF1^{mCherry-} SI LP SFB Th17 cells from *Tcf7*^{mCherry}/*Il17a*^{GFP} mice. Two independent experiments, n = 4 mice/group.
- (H) TCF1^{mCherry} and IL-10^{Venus} expression in SI LP SFB Th17 cells (TCR β ⁺CD4⁺IL-17^{GFP+}) from *Tcf7*^{mCherry}/*Il17a*^{GFP}/*Il10*^{Venus} mice. Two independent experiments, n = 3 mice/group.
- (I) TCF1^{mCherry+}IL-17A^{GFP+} CD4⁺ T cells were purified from SI LP of *Tcf7*^{mCherry}/*Il17a*^{GFP} mice and adoptively transferred into SFB-colonized WT mice. TCF1 and IL-17 expression in transferred cells in SI LP was analyzed on day 2 and day 14 after transfer. Cumulative from several independent experiments, n = 5 mice/group.
- (J) TCF1^{mCherry+}IL-17^{GFP+}IL-10^{Venus-} Th17 cells were FACS-purified from SI LP of SFB-colonized or LI LP of *Citrobacter rodentium* (*Crod*) infected mice and stimulated *in vitro* for 4 days as described in STAR Methods. (Left) IL-10^{Venus} and IL-17^{GFP} expression. (Right) Proportion of IL-10^{Venus+} cells in IL-17^{GFP+} Th17 cells. Three independent experiments, n = 2–7 mice/group.
- (K) PCA plot of bulk RNA-seq analysis of TCF1^{mCherry+} and TCF1^{mCherry-}IL-17^{GFP+} Th17 cells from SI LP of SFB-colonized or LI LP of *Citrobacter rodentium*-infected (*Crod*) mice. One experiment, n = 2–4 mice/group.
- (L) Number of differentially expressed genes (DEGs) in indicated pairwise comparisons from the RNA-seq in (K). One experiment, n = 2–4 mice/group.
- (M) Gene set enrichment analysis of genes (left) elevated in TCF1⁺ SFB Th17 cells compared with genes elevated in total SFB Th17 cells or (right) elevated in TCF1⁺ *Crod* Th17 cells compared with total *Crod* Th17 cells.
- (N) Heatmap of DEGs between TCF1⁺ SFB and TCF1⁺ *Crod* Th17 cells. SFB core signature anti-inflammatory genes in blue and inflammatory genes in red are marked.
- (O) Quantitative PCR for selected SFB Th17 signature genes from samples in (K).
- (P) TCF1^{mCherry+}IL-17^{GFP+}IL-10^{Venus-} Th17 cells were purified from SI LP of SFB-colonized mice and stimulated *in vitro* with or without 10 ng/mL IL-1 β and 10 ng/mL IL-23 for 4 days. (Left) IL-10^{Venus} and IL-17^{GFP} expression. (Right) Proportion of IL-10^{Venus+} cells in TCF1^{mCherry+}IL-17^{GFP+} Th17 cells. Two independent experiments, each dot represents a technical replicate.
- (Q) IFN- γ ELISA from *in vitro* cultures in (P). Two independent experiments, each dot represents a technical replicate. See also Figure S6.

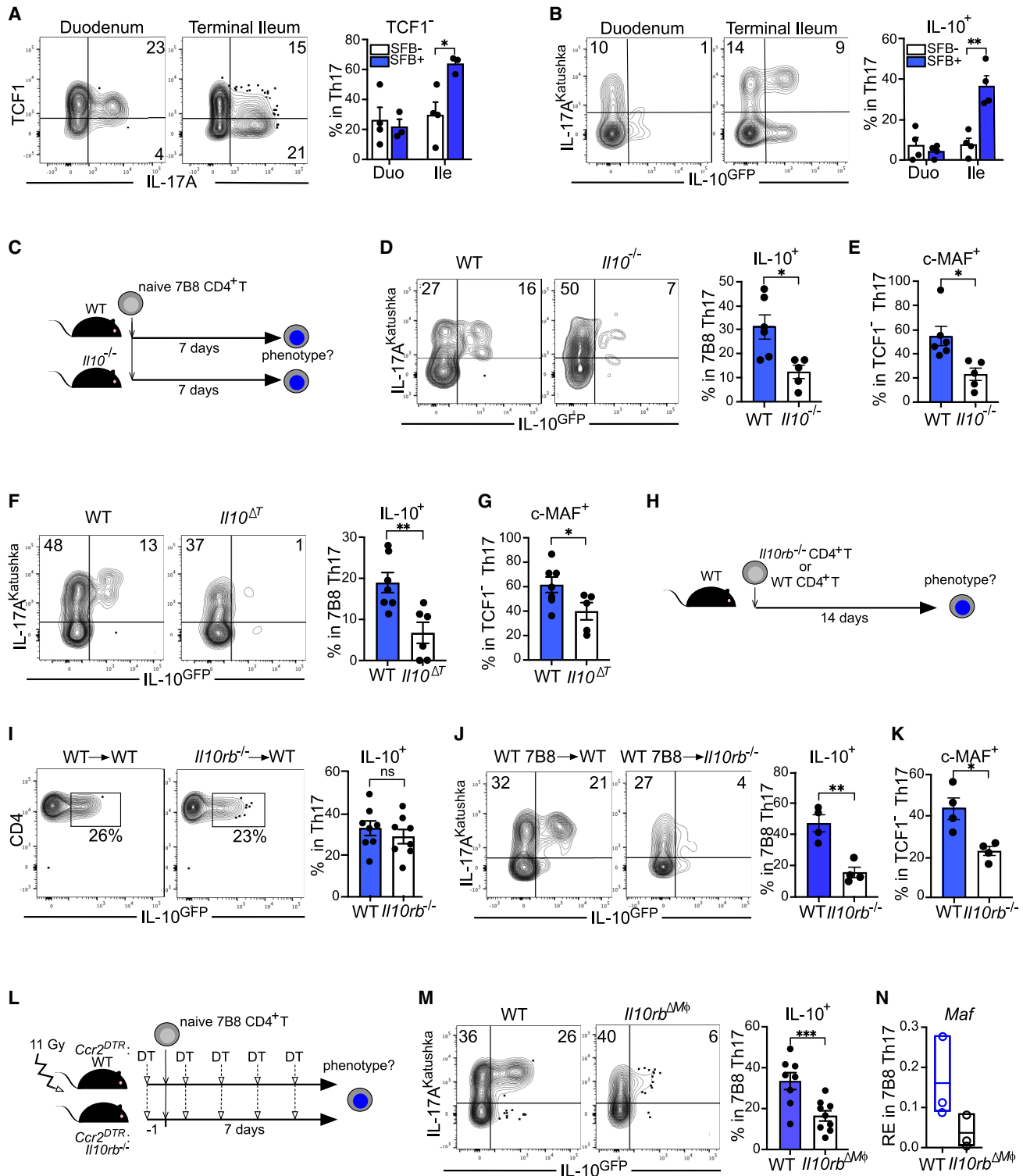


Figure 7. IL-10 signaling in intestinal macrophages drives generation of anti-inflammatory commensal Th17 cells in the terminal ileum

(A) Intracellular staining for TCF1 and IL-17 in duodenum (Duo) and terminal ileum (Ile) SI LP of SFB-colonized and SFB-negative WT mice. (Left) Representative FACS plots from SFB-colonized mice, gated on CD4⁺ T cells. (Right) Proportion of TCF1⁻ effector cells within Th17 cells. Two independent experiments, n = 3 mice/group.

(B) Distribution of IL-10^{GFP+} Th17 cells in the SI LP. (Left) Representative plots from duodenum and terminal ileum of SFB-colonized Il10^{eGFP}/Il17a^{Katushka}/Foxp3^{mRFP} mice, gated on CD4⁺ T cells. (Right) Proportion of IL-10^{GFP+} cells within Th17 cells. Two independent experiments, n = 4 mice/group.

(legend continued on next page)

Therefore, commensal Th17 cells may possess additional mechanisms for maintaining T cell homeostasis, besides IL-10.

c-MAF plays divergent roles in the specialization of IL-17-producing T cells. c-MAF is not essential for ROR γ expression in Th17 cells and Th17 cell differentiation.³⁸ However, c-MAF is activated early during Th17 cell polarization together with T_H17-defining transcription factors and can act as a negative regulator.³⁶ In contrast, c-MAF is required for the development of ROR γ t⁺ Treg cells and for the specialization of IL-17⁺ $\gamma\delta$ T cells, where it acts as an activator.^{38,58,59} Regardless of its overall role, c-MAF is linked to positive regulation of IL-10 expression in T cells, including Th17 cells.^{36,58} Here, we find that c-MAF is required for the production of IL-10 by commensal Th17 cells. Moreover, c-MAF was required for the maintenance of the anti-inflammatory program of commensal Th17 cells. This included the expression of tissue-repair factors and co-inhibitory receptors. Th17-cell-specific ablation of c-MAF led to expansion of IFN- γ ⁺ Th17 cells and IL-17⁻ ex-Th17 cells with a pro-inflammatory Th1 phenotype. Thus, c-MAF may also maintain anti-inflammatory phenotype of commensal Th17 cells by restricting inflammatory cytokines and Th17 cell plasticity.

We find that IL-10⁺ Th17 cells were only present in the terminal ileum. Therefore, signals in this location likely mediate the induction or maintenance of their anti-inflammatory program. We previously showed that intestinal epithelial cells and iM ϕ play crucial roles in SFB Th17 cell induction.^{54,60} Here, we find that ablation of IL-10R β in macrophages perturbs induction of anti-inflammatory Th17 cells but does not affect overall Th17 cell differentiation. Therefore, iM ϕ are required for the induction or maintenance of anti-inflammatory Th17 cells. IL-10R β signaling in macrophages is crucial for maintenance of intestinal homeostasis.⁵⁵ Our data suggest that maintenance of anti-inflammatory commensal Th17 cells may contribute to the mechanisms by which resident macrophages suppress gut inflammation. Although the exact source of IL-10 required for iM ϕ activation remains to be ascertained, we find that IL-10 from CD4⁺ T cells is required for the presence of IL-10⁺ Th17 cells. Both Foxp3⁺ Treg cells and Foxp3⁻ Tr1 cells can produce IL-10, thus, establishing

an interdependent network of IL-10-producing CD4⁺ T cells in mucosal homeostasis.

Pathogens induce quantitatively different T cell responses in the context of acute versus chronic infection. Whether commensals engage adaptive immunity in an acute or chronic manner is not known. In agreement with the expression of IL-10 and generally inhibitory or non-responsive program, commensal Th17 cells closely resembled exhausted T cells induced during chronic infection. Therefore, in terms of T cell responses, presence of commensals resembles chronic infection. We also found substantial heterogeneity of commensal Th17 cells and the existence of a precursor TCF1⁺ Th17 cell population in the SI LP that generates TCF1⁻IL-10⁺ Th17 cells. Similar TCF1⁺ progenitor CD4⁺ and CD8⁺ T cells maintain TCF⁻ effector responses in the context of chronic viral infections,^{61,62} further underscoring the similarities between homeostatic commensal and chronic infection T cell responses. SFB TCF1⁺ progenitor Th17 cells were transcriptionally distinct from TCF1⁺ Th17 cells during *Crod* infection. Even though they retained the potential to generate inflammatory Th17 cells, intestinal TCF1⁺ Th17 cells closely resembled their TCF1⁻ counterparts. Therefore, they were already poised toward an anti-inflammatory program. Our results suggest that this happens in the SI LP under the control of the local microenvironment. The specific signals controlling this transition, as well as the earliest events leading to the establishment of the SFB Th17 cell differentiation program will be important to elucidate in future studies.

TCF1⁻ commensal Th17 cells possessed inhibitory or activated phenotype and contained both IL-10⁺ and IL-10⁻ Th17 cells. Therefore, individual commensals generate heterogeneous T cell responses. We identified two unique subsets of IL-10⁺ Th17 cells, both of which required c-MAF for IL-10 production. Whether these two subsets perform different functions or whether commensal Th17 subsets with distinct functions co-exist, will be important to elucidate in future studies.

Our results describe an inherent heterogeneity of the Th17 cell response to commensal microbes and show that such response may function not only in antigen-specific control of the inducing commensal but also in general regulation of intestinal T cells and in maintaining anti-inflammatory tone in the intestinal mucosa.

(C–E) Naive SFB-specific 7B8.Ly5.1 triple reporter splenic CD4⁺ T cells were adoptively transferred into SFB-colonized Ly5.2 WT or *Il10*^{-/-} mice (C). Expression of IL-10 (GFP) (D) and c-MAF (intracellular staining) (E) in SI LP 1 week after transfer. FACS plots in (D) gated on Ly5.1⁺ CD4⁺ T cells. Bar plots in (D) gated on IL-17^{Katushka} Th17 cells. Bar plots in (E) gated on IL-17⁺ transferred 7B8 Th17 cells. Cumulative of three independent experiments, n = 5–6 mice/group.

(F and G) Naive SFB-specific 7B8.Ly5.1 triple reporter splenic CD4⁺ T cells were adoptively transferred into SFB-colonized WT or *Cd4*^{Cre}/*Il10*^{flx/flx} (*Il10*^{-/-}) mice. Expression of IL-10 (GFP) (F) and c-MAF (G) in SI LP 1 week after transfer. FACS plots in (F) gated on Ly5.1⁺ 7B8 CD4 T cells. Bar plots gated on IL-17^{Katushka} (F) or IL-17⁺ (G) transferred 7B8 Th17 cells. Cumulative of two independent experiments, n = 6–7 mice/group.

(H) Experimental schematic. Naive splenic CD4⁺ T cells were purified from *Il10*^{GFP}/*Il17a*^{Katushka}/*Foxp3*^{mRFP} (Ly5.2) WT or *Il10rb*^{-/-} mice and adoptively transferred into SFB-colonized Ly5.1 WT mice.

(I) IL-10 and c-MAF expression in transferred Th17 cells in SI LP 2 weeks after transfer in the mice in (H). FACS plots and bar plots gated on Ly5.2⁺TCR β ⁺ CD4⁺Foxp3^{mRFP}-IL-17^{Katushka} Th17 cells. Cumulative of four independent experiments, n = 8 mice/group.

(J and K) Naive SFB-specific 7B8.Ly5.1 triple reporter splenic CD4⁺ T cells were adoptively transferred into SFB-colonized Ly5.2 WT or *Il10rb*^{-/-} mice. IL-10 (GFP) (J) and c-MAF (K) expression in SI LP Th17 cells 1 week after transfer. FACS plots gated on Ly5.1⁺ transferred 7B8 T cells. Bar plots further gated on IL-17^{Katushka} (J) or IL-17⁺ (K) transferred 7B8 Th17 cells. Cumulative of two independent experiments, n = 4 mice/group.

(L) Experimental schematic. Naive SFB-specific 7B8.Ly5.1 triple reporter splenic CD4⁺ T cells were adoptively transferred into diphtheria toxin (DT) treated SFB-colonized Ly5.2 WT BM chimeras, reconstituted with 1:1 mix of BM from *Ccr2*^{DTR} mice and either WT or *Il10rb*^{-/-} mice. DT treatment was performed to deplete *Ccr2*^{DTR} macrophages as described in [STAR Methods](#).

(M) IL-10 (GFP) expression in SI LP 1 week after transfer in the mice in (L). FACS plots gated on Ly5.1⁺ transferred 7B8 CD4⁺ T cells. Bar plots further gated on IL-17^{Katushka} transferred 7B8 Th17 cells. Cumulative of two independent experiments, n = 8–9 mice/group.

(N) Quantitative PCR of *Maf* transcripts in FACS-purified transferred SI LP 7B8 Th17 cells (Ly5.1⁺TCR β ⁺CD4⁺Foxp3^{mRFP}-IL-17^{GFP}) from the mice in (L). Cumulative of two independent experiments, n = 3 mice/group.

See also [Figure S7](#).

Limitations of the study

The SFB-induced core Th17 cell program we investigated here was restricted to DEGs compared with at least three other Th17 cell datasets and may have excluded potential functionally important genes. One example is *I122*, which is an important effector cytokine for intestinal Th17 cells but is also highly expressed in SI and LI *Citrobacter*-induced Th17 cells. It was therefore excluded from our analysis. Of note, despite loss of the core anti-inflammatory program, *I122* and IL-22 expression by SFB Th17 cells does not decrease in absence of c-MAF. Therefore, IL-22 is not part of the c-MAF controlled anti-inflammatory program in SFB Th17 cells. Although we demonstrate that commensal-specific Th17 cells can regulate T cell responses *in vitro* and *in vivo*, their specific role in relation to other regulatory mechanisms in the gut in various contexts, e.g., suppression of pathogen-induced T cells or intestinal inflammation, will be important to investigate. Our study was also mostly restricted to SFB-specific Th17 cells. Even though we found that *Bifidobacterium adolescentis*-induced intestinal Th17 cells also express IL-10 and c-MAF, we did not test whether they possess similar anti-inflammatory functional activities. Finally, like similar prior studies, our study was limited to the effects of mouse or human commensal microbes in animal models. How human microbes affect mucosal immunity in human hosts remains to be studied.

STAR★METHODS

Detailed methods are provided in the online version of this paper and include the following:

- KEY RESOURCES TABLE
- RESOURCE AVAILABILITY
 - Lead contact
 - Materials availability
 - Data and code availability
- EXPERIMENTAL MODEL AND STUDY PARTICIPANT DETAILS
 - *In vivo* animal studies
 - Bacterial colonization and infection
 - Transfer colitis
 - *In vivo* suppression assay
 - Adoptive transfers
 - Migration assays
 - Mixed bone marrow chimeras
- METHOD DETAILS
 - *In vitro* suppression assay
 - Lymphocyte isolation from intestine and flow cytometry
 - *In vitro* culture
 - Lipocalin-2 ELISA
 - IFN- γ ELISA
 - Quantitative PCR
 - Bulk RNA-sequencing and analysis
 - Gene set enrichment analysis (GSEA)
 - Identification of c-MAF target genes
 - Single cell RNA-sequencing and analysis
- QUANTIFICATION AND STATISTICAL ANALYSIS

SUPPLEMENTAL INFORMATION

Supplemental information can be found online at <https://doi.org/10.1016/j.immuni.2023.11.003>.

ACKNOWLEDGMENTS

We thank Samuel Huber and Nicola Gagliani (UKE) for providing key mouse lines. We thank Steve Reiner for helpful advice. We thank members of the Ivanov lab for technical help. This work was supported by funding from NIH (DK098378, AI144808, AI163069, and AI146817) and Burroughs Wellcome Fund (PATH1019125) to I.I.I. L.B. was partially supported by a fellowship from the German Research Foundation (DFG) (BR 6094/1-1). H.H.W. acknowledges funding from NSF (MCB-2025515), NIH (R01AI132403, R01DK118044, and R01EB031935), Burroughs Wellcome Fund (PATH1016691), and the Irma T. Hirschl Trust.

AUTHOR CONTRIBUTIONS

Conceptualization, L.B. and I.I.I.; methodology, L.B., A.T., Y.H., C.R., and I.I.I.; software, Y.H., A.T., and H.H.W.; formal analysis, L.B., A.T., Y.H., and I.I.I.; investigation, L.B., A.T., Y.H., M.E., and C.R.; resources, H.H.W. and I.I.I.; data curation, L.B., A.T., and Y.H.; writing – original draft, L.B. and I.I.I.; writing – review & editing, L.B. and I.I.I.; supervision, I.I.I.; funding acquisition, I.I.I.

DECLARATION OF INTERESTS

H.H.W. is a scientific advisor of SNIPR Biome, Kingdom Supercultures and Fitbiotics, who were not involved in the study.

INCLUSION AND DIVERSITY

We support inclusive, diverse, and equitable conduct of research.

Received: March 13, 2023

Revised: August 4, 2023

Accepted: November 5, 2023

Published: November 30, 2023

REFERENCES

1. Ivanov, I.I., Tuganbaev, T., Skelly, A.N., and Honda, K. (2022). T cell responses to the microbiota. *Annu. Rev. Immunol.* **40**, 559–587.
2. Hooper, L.V., Littman, D.R., and Macpherson, A.J. (2012). Interactions between the microbiota and the immune system. *Science* **336**, 1268–1273.
3. Lathrop, S.K., Bloom, S.M., Rao, S.M., Nutsch, K., Lio, C.W., Santacruz, N., Peterson, D.A., Stappenbeck, T.S., and Hsieh, C.S. (2011). Peripheral education of the immune system by colonic commensal microbiota. *Nature* **478**, 250–254.
4. Atarashi, K., Tanoue, T., Oshima, K., Suda, W., Nagano, Y., Nishikawa, H., Fukuda, S., Saito, T., Narushima, S., Hase, K., et al. (2013). Treg induction by a rationally selected mixture of Clostridia strains from the human microbiota. *Nature* **500**, 232–236.
5. Nutsch, K.M., and Hsieh, C.S. (2012). T cell tolerance and immunity to commensal bacteria. *Curr. Opin. Immunol.* **24**, 385–391.
6. Ivanov, I.I., Atarashi, K., Manel, N., Brodie, E.L., Shima, T., Karaoz, U., Wei, D., Goldfarb, K.C., Santee, C.A., Lynch, S.V., et al. (2009). Induction of intestinal Th17 cells by segmented filamentous bacteria. *Cell* **139**, 485–498.
7. Ivanov, I.I., Frutos, L., Manel, N., Yoshinaga, K., Rifkin, D.B., Sartor, R.B., Finlay, B.B., and Littman, D.R. (2008). Specific microbiota direct the differentiation of IL-17-producing T-helper cells in the mucosa of the small intestine. *Cell Host Microbe* **4**, 337–349.
8. Atarashi, K., Tanoue, T., Ando, M., Kamada, N., Nagano, Y., Narushima, S., Suda, W., Imaoka, A., Setoyama, H., Nagamori, T., et al. (2015). Th17 cell induction by adhesion of microbes to intestinal epithelial cells. *Cell* **163**, 367–380.

9. Gaboriau-Routhiau, V., Rakotobe, S., Lécuyer, E., Mulder, I., Lan, A., Bridonneau, C., Rochet, V., Pisi, A., De Paepe, M., Brandi, G., et al. (2009). The key role of segmented filamentous bacteria in the coordinated maturation of gut helper T cell responses. *Immunity* *31*, 677–689.
10. Kumar, P., Monin, L., Castillo, P., Elsegeiny, W., Horne, W., Eddens, T., Vikram, A., Good, M., Schoenborn, A.A., Bibby, K., et al. (2016). Intestinal interleukin-17 receptor signaling mediates reciprocal control of the gut microbiota and autoimmune inflammation. *Immunity* *44*, 659–671.
11. Ghoreschi, K., Laurence, A., Yang, X.P., Tato, C.M., McGeachy, M.J., Konkel, J.E., Ramos, H.L., Wei, L., Davidson, T.S., Bouladoux, N., et al. (2010). Generation of pathogenic T(H)17 cells in the absence of TGF-beta signalling. *Nature* *467*, 967–971.
12. Esplugues, E., Huber, S., Gagliani, N., Hauser, A.E., Town, T., Wan, Y.Y., O'Connor, W., Jr., Rongvaux, A., Van Rooijen, N., Haberman, A.M., et al. (2011). Control of TH17 cells occurs in the small intestine. *Nature* *475*, 514–518.
13. Gaublot, J.T., Yosef, N., Lee, Y., Gertner, R.S., Yang, L.V., Wu, C., Pandolfi, P.P., Mak, T., Satija, R., Shalek, A.K., et al. (2015). Single-cell genomics unveils critical regulators of Th17 cell pathogenicity. *Cell* *163*, 1400–1412.
14. El-Behi, M., Ciric, B., Dai, H., Yan, Y., Cullimore, M., Safavi, F., Zhang, G.X., Dittel, B.N., and Rostami, A. (2011). The encephalitogenicity of T(H)17 cells is dependent on IL-1- and IL-23-induced production of the cytokine GM-CSF. *Nat. Immunol.* *12*, 568–575.
15. McGeachy, M.J., Bak-Jensen, K.S., Chen, Y., Tato, C.M., Blumenschein, W., McClanahan, T., and Cua, D.J. (2007). TGF-beta and IL-6 drive the production of IL-17 and IL-10 by T cells and restrain T(H)-17 cell-mediated pathology. *Nat. Immunol.* *8*, 1390–1397.
16. Leppkes, M., Becker, C., Ivanov, I.I., Hirth, S., Wirtz, S., Neufert, C., Pouly, S., Murphy, A.J., Valenzuela, D.M., Yancopoulos, G.D., et al. (2009). RORgamma-expressing Th17 cells induce murine chronic intestinal inflammation via redundant effects of IL-17A and IL-17F. *Gastroenterology* *136*, 257–267.
17. Alexander, M., Ang, Q.Y., Nayak, R.R., Bustion, A.E., Sandy, M., Zhang, B., Upadhyay, V., Pollard, K.S., Lynch, S.V., and Turnbaugh, P.J. (2022). Human gut bacterial metabolism drives Th17 activation and colitis. *Cell Host Microbe* *30*, 17–30.e9.
18. Basu, R., O'Quinn, D.B., Silberger, D.J., Schoeb, T.R., Fouser, L., Ouyang, W., Hatton, R.D., and Weaver, C.T. (2012). Th22 cells are an important source of IL-22 for host protection against enteropathogenic bacteria. *Immunity* *37*, 1061–1075.
19. Maxwell, J.R., Zhang, Y., Brown, W.A., Smith, C.L., Byrne, F.R., Fiorino, M., Stevens, E., Bigler, J., Davis, J.A., Rottman, J.B., et al. (2015). Differential roles for interleukin-23 and interleukin-17 in intestinal immunoregulation. *Immunity* *43*, 739–750.
20. Lee, J.S., Tato, C.M., Joyce-Shaikh, B., Gulen, M.F., Cayatte, C., Chen, Y., Blumenschein, W.M., Judo, M., Ayanoglu, G., McClanahan, T.K., et al. (2015). Interleukin-23-independent IL-17 production regulates intestinal epithelial permeability. *Immunity* *43*, 727–738.
21. Fauny, M., Moulin, D., D'Amico, F., Netter, P., Petitpain, N., Arnone, D., Jouzeau, J.Y., Loeuille, D., and Peyrin-Biroulet, L. (2020). Paradoxical gastrointestinal effects of interleukin-17 blockers. *Ann. Rheum. Dis.* *79*, 1132–1138.
22. Gagliani, N., Amezcua Vesely, M.C., Iseppon, A., Brockmann, L., Xu, H., Palm, N.W., de Zoete, M.R., Licona-Limón, P., Paiva, R.S., Ching, T., et al. (2015). Th17 cells transdifferentiate into regulatory T cells during resolution of inflammation. *Nature* *523*, 221–225.
23. Schnell, A., Littman, D.R., and Kuchroo, V.K. (2023). TH17 cell heterogeneity and its role in tissue inflammation. *Nat. Immunol.* *24*, 19–29.
24. Omenetti, S., Bussi, C., Metidji, A., Iseppon, A., Lee, S., Tolaini, M., Li, Y., Kelly, G., Chakravarty, P., Shoaie, S., et al. (2019). The intestine harbors functionally distinct homeostatic tissue-resident and inflammatory Th17 cells. *Immunity* *51*, 77–89.e6.
25. Chihara, N., Madi, A., Kondo, T., Zhang, H., Acharya, N., Singer, M., Nyman, J., Marjanovic, N.D., Kowalczyk, M.S., Wang, C., et al. (2018). Induction and transcriptional regulation of the co-inhibitory gene module in T cells. *Nature* *558*, 454–459.
26. Crawford, A., Angelosanto, J.M., Kao, C., Doering, T.A., Odorizzi, P.M., Barnett, B.E., and Wherry, E.J. (2014). Molecular and transcriptional basis of CD4⁺ T cell dysfunction during chronic infection. *Immunity* *40*, 289–302.
27. Martinez, G.J., Pereira, R.M., Åijö, T., Kim, E.Y., Marangoni, F., Pipkin, M.E., Togher, S., Heissmeyer, V., Zhang, Y.C., Crotty, S., et al. (2015). The transcription factor NFAT promotes exhaustion of activated CD8⁺ T cells. *Immunity* *42*, 265–278.
28. Alfei, F., Kanev, K., Hofmann, M., Wu, M., Ghoneim, H.E., Roelli, P., Utzschneider, D.T., von Hoesslin, M., Cullen, J.G., Fan, Y., et al. (2019). TOX reinforces the phenotype and longevity of exhausted T cells in chronic viral infection. *Nature* *571*, 265–269.
29. Aschenbrenner, D., Foglierini, M., Jarrossay, D., Hu, D., Weiner, H.L., Kuchroo, V.K., Lanzavecchia, A., Notarbartolo, S., and Sallusto, F. (2018). An immunoregulatory and tissue-residency program modulated by c-MAF in human TH17 cells. *Nat. Immunol.* *19*, 1126–1136.
30. Cao, S., Liu, J., Song, L., and Ma, X. (2005). The protooncogene c-Maf is an essential transcription factor for IL-10 gene expression in macrophages. *J. Immunol.* *174*, 3484–3492.
31. Xu, J., Yang, Y., Qiu, G., Lal, G., Wu, Z., Levy, D.E., Ochando, J.C., Bromberg, J.S., and Ding, Y. (2009). c-Maf regulates IL-10 expression during Th17 polarization. *J. Immunol.* *182*, 6226–6236.
32. Pot, C., Jin, H., Awasthi, A., Liu, S.M., Lai, C.Y., Madan, R., Sharpe, A.H., Karp, C.L., Miaw, S.C., Ho, I.C., et al. (2009). Cutting edge: il-27 induces the transcription factor c-Maf, cytokine IL-21, and the costimulatory receptor ICOS that coordinately act together to promote differentiation of IL-10-producing Tr1 cells. *J. Immunol.* *183*, 797–801.
33. Apetoh, L., Quintana, F.J., Pot, C., Joller, N., Xiao, S., Kumar, D., Burns, E.J., Sherr, D.H., Weiner, H.L., and Kuchroo, V.K. (2010). The aryl hydrocarbon receptor interacts with c-Maf to promote the differentiation of type 1 regulatory T cells induced by IL-27. *Nat. Immunol.* *11*, 854–861.
34. Zhu, C., Sakuishi, K., Xiao, S., Sun, Z., Zaghouani, S., Gu, G., Wang, C., Tan, D.J., Wu, C., Rangachari, M., et al. (2015). An IL-27/NFIL3 signalling axis drives Tim-3 and IL-10 expression and T-cell dysfunction. *Nat. Commun.* *6*, 6072.
35. Ridley, M.L., Fleskens, V., Roberts, C.A., Lalnunhlimi, S., Alnesf, A., O'Byrne, A.M., Steel, K.J.A., Povoleri, G.A.M., Sumner, J., Lavender, P., et al. (2020). IKZF3/Aiolos is associated with but not sufficient for the expression of IL-10 by CD4(+) T cells. *J. Immunol.* *204*, 2940–2948.
36. Ciofani, M., Madar, A., Galan, C., Sellars, M., Mace, K., Pauli, F., Agarwal, A., Huang, W., Parkhurst, C.N., Muratet, M., et al. (2012). A validated regulatory network for Th17 cell specification. *Cell* *151*, 289–303.
37. Tan, T.G., Sefik, E., Geva-Zatorsky, N., Kua, L., Naskar, D., Teng, F., Pisman, L., Ortiz-Lopez, A., Jupp, R., Wu, H.J., et al. (2016). Identifying species of symbiont bacteria from the human gut that, alone, can induce intestinal Th17 cells in mice. *Proc. Natl. Acad. Sci. USA* *113*, E8141–E8150.
38. Zuberbuehler, M.K., Parker, M.E., Wheaton, J.D., Espinosa, J.R., Salzler, H.R., Park, E., and Ciofani, M. (2019). The transcription factor c-Maf is essential for the commitment of IL-17-producing $\gamma\delta$ T cells. *Nat. Immunol.* *20*, 73–85.
39. Neumann, C., Blume, J., Roy, U., Teh, P.P., Vasanthakumar, A., Beller, A., Liao, Y., Heinrich, F., Arenzana, T.L., Hackney, J.A., et al. (2019). c-Maf-dependent T(reg) cell control of intestinal TH17 cells and IgA establishes host-microbiota homeostasis. *Nat. Immunol.* *20*, 471–481.
40. Hu, D., Notarbartolo, S., Croonenborghs, T., Patel, B., Cialic, R., Yang, T.H., Aschenbrenner, D., Andersson, K.M., Gattomo, M., Pham, M., et al. (2017). Transcriptional signature of human pro-inflammatory TH17 cells identifies reduced IL10 gene expression in multiple sclerosis. *Nat. Commun.* *8*, 1600.
41. Goto, Y., Panea, C., Nakato, G., Cebula, A., Lee, C., Diez, M.G., Laufer, T.M., Ignatowicz, L., and Ivanov, I.I. (2014). Segmented filamentous bacteria antigens presented by intestinal dendritic cells drive mucosal Th17 cell differentiation. *Immunity* *40*, 594–607.
42. Farkas, A.M., Panea, C., Goto, Y., Nakato, G., Galan-Diez, M., Narushima, S., Honda, K., and Ivanov, I.I. (2015). Induction of Th17 cells by segmented

- filamentous bacteria in the murine intestine. *J. Immunol. Methods* **421**, 104–111.
43. Sano, T., Huang, W., Hall, J.A., Yang, Y., Chen, A., Gavzy, S.J., Lee, J.Y., Ziel, J.W., Miraldi, E.R., Domingos, A.I., et al. (2015). An IL-23R/IL-22 circuit regulates epithelial serum amyloid A to promote local effector Th17 responses. *Cell* **163**, 381–393.
44. Jenstad, H., Ericsson, A., Johansson-Lindbom, B., Svensson, M., Marsal, J., Mack, M., Picarella, D., Soler, D., Marquez, G., Briskin, M., et al. (2006). Gut-associated lymphoid tissue-primed CD4⁺ T cells display CCR9-dependent and -independent homing to the small intestine. *Blood* **107**, 3447–3454.
45. Woodward Davis, A.S., Roozen, H.N., Dufort, M.J., DeBerg, H.A., Delaney, M.A., Mair, F., Erickson, J.R., Slichter, C.K., Berkson, J.D., Klock, A.M., et al. (2019). The human tissue-resident CCR5(+) T cell compartment maintains protective and functional properties during inflammation. *Sci. Transl. Med.* **11**.
46. Iijima, N., and Iwasaki, A. (2014). T cell memory. A local macrophage chemokine network sustains protective tissue-resident memory CD4 T cells. *Science* **346**, 93–98.
47. Turner, D.L., and Farber, D.L. (2014). Mucosal resident memory CD4 T cells in protection and immunopathology. *Front. Immunol.* **5**, 331.
48. Wagner, A., Wang, C., Fessler, J., DeTomaso, D., Avila-Pacheco, J., Kaminski, J., Zaghouni, S., Christian, E., Thakore, P., Schellhaas, B., et al. (2021). Metabolic modeling of single Th17 cells reveals regulators of autoimmunity. *Cell* **184**, 4168–4185.e21.
49. Schnell, A., Huang, L., Singer, M., Singaraju, A., Barilla, R.M., Regan, B.M.L., Bollhagen, A., Thakore, P.I., Dionne, D., Delorey, T.M., et al. (2021). Stem-like intestinal Th17 cells give rise to pathogenic effector T cells during autoimmunity. *Cell* **184**, 6281–6298.e23.
50. Nish, S.A., Zens, K.D., Kratchmarov, R., Lin, W.W., Adams, W.C., Chen, Y.H., Yen, B., Rothman, N.J., Bhandoola, A., Xue, H.H., et al. (2017). CD4⁺ T cell effector commitment coupled to self-renewal by asymmetric cell divisions. *J. Exp. Med.* **214**, 39–47.
51. Groux, H., O’Garra, A., Bigler, M., Rouleau, M., Antonenko, S., de Vries, J.E., and Roncarolo, M.G. (1997). A CD4⁺ T-cell subset inhibits antigen-specific T-cell responses and prevents colitis. *Nature* **389**, 737–742.
52. Brockmann, L., Gagliani, N., Steglich, B., Giannou, A.D., Kempski, J., Pelczar, P., Geffken, M., Mfarrej, B., Huber, F., Herkel, J., et al. (2017). IL-10 receptor signaling is essential for TR1 cell function in vivo. *J. Immunol.* **198**, 1130–1141.
53. Chaudhry, A., Samstein, R.M., Treuting, P., Liang, Y., Pils, M.C., Heinrich, J.M., Jack, R.S., Wunderlich, F.T., Brünning, J.C., Müller, W., et al. (2011). Interleukin-10 signaling in regulatory T cells is required for suppression of Th17 cell-mediated inflammation. *Immunity* **34**, 566–578.
54. Panea, C., Farkas, A.M., Goto, Y., Abdollahi-Roodsaz, S., Lee, C., Koscsó, B., Gowda, K., Hohl, T.M., Bogunovic, M., and Ivanov, I.I. (2015). Intestinal monocyte-derived macrophages control commensal-specific Th17 responses. *Cell Rep.* **12**, 1314–1324.
55. Zsigmond, E., Bernshtein, B., Friedlander, G., Walker, C.R., Yona, S., Kim, K.W., Brenner, O., Krauthgamer, R., Varol, C., Müller, W., et al. (2014). Macrophage-restricted interleukin-10 receptor deficiency, but not IL-10 deficiency, causes severe spontaneous colitis. *Immunity* **40**, 720–733.
56. Shih, V.F., Cox, J., Kljavin, N.M., Dengler, H.S., Reichelt, M., Kumar, P., Rangell, L., Kolls, J.K., Diehl, L., Ouyang, W., et al. (2014). Homeostatic IL-23 receptor signaling limits Th17 response through IL-22-mediated containment of commensal microbiota. *Proc. Natl. Acad. Sci. USA* **111**, 13942–13947.
57. Kawano, Y., Edwards, M., Huang, Y., Bilate, A.M., Araujo, L.P., Tanoue, T., Atarashi, K., Ladinsky, M.S., Reiner, S.L., Wang, H.H., et al. (2022). Microbiota imbalance induced by dietary sugar disrupts immune-mediated protection from metabolic syndrome. *Cell* **185**, 3501–3519.e20.
58. Xu, M., Pokrovskii, M., Ding, Y., Yi, R., Au, C., Harrison, O.J., Galan, C., Belkaid, Y., Bonneau, R., and Littman, D.R. (2018). c-MAF-dependent regulatory T cells mediate immunological tolerance to a gut pathobiont. *Nature* **554**, 373–377.
59. Wheaton, J.D., Yeh, C.H., and Ciofani, M. (2017). Cutting edge: c-Maf is required for regulatory T cells to adopt ROR γ t(+) and follicular phenotypes. *J. Immunol.* **199**, 3931–3936.
60. Ladinsky, M.S., Araujo, L.P., Zhang, X., Veltri, J., Galan-Diez, M., Soualhi, S., Lee, C., Irie, K., Pinker, E.Y., Narushima, S., et al. (2019). Endocytosis of commensal antigens by intestinal epithelial cells regulates mucosal T cell homeostasis. *Science* **363**, eaat4042.
61. Xia, Y., Sandor, K., Pai, J.A., Daniel, B., Raju, S., Wu, R., Hsiung, S., Qi, Y., Yangdon, T., Okamoto, M., et al. (2022). BCL6-dependent TCF-1(+) progenitor cells maintain effector and helper CD4(+) T cell responses to persistent antigen. *Immunity* **55**, 1200–1215.e6.
62. Utzschneider, D.T., Charmoy, M., Chennupati, V., Pousse, L., Ferreira, D.P., Calderon-Copete, S., Danilo, M., Alfei, F., Hofmann, M., Wieland, D., et al. (2016). T cell factor 1-expressing memory-like CD8(+) T cells sustain the immune response to chronic viral infections. *Immunity* **45**, 415–427.
63. Umesaki, Y., Okada, Y., Matsumoto, S., Imaoka, A., and Setoyama, H. (1995). Segmented filamentous bacteria are indigenous intestinal bacteria that activate intraepithelial lymphocytes and induce MHC class II molecules and fucosyl asialo GM1 glycolipids on the small intestinal epithelial cells in the ex-germ-free mouse. *Microbiol. Immunol.* **39**, 555–562.
64. Esterházy, D., Canesso, M.C.C., Mesin, L., Muller, P.A., de Castro, T.B.R., Lockhart, A., ElJalby, M., Faria, A.M.C., and Mucida, D. (2019). Compartmentalized gut lymph node drainage dictates adaptive immune responses. *Nature* **569**, 126–130.
65. Huang, Y., Sheth, R.U., Zhao, S., Cohen, L.A., Dabaghi, K., Moody, T., Sun, Y., Ricaurte, D., Richardson, M., Velez-Cortes, F., et al. (2023). High-throughput microbial culturomics using automation and machine learning. *Nat. Biotechnol.* **41**, 1424–1433.
66. Vaaben, T.H., Vazquez-Urbe, R., and Sommer, M.O.A. (2022). Characterization of eight bacterial biosensors for microbial diagnostic and therapeutic applications. *ACS Synth. Biol.* **11**, 4184–4192.
67. Roers, A., Siewe, L., Strittmatter, E., Deckert, M., Schlüter, D., Stenzel, W., Gruber, A.D., Krieg, T., Rajewsky, K., and Müller, W. (2004). T cell-specific inactivation of the interleukin 10 gene in mice results in enhanced T cell responses but normal innate responses to lipopolysaccharide or skin irritation. *J. Exp. Med.* **200**, 1289–1297.
68. Hohl, T.M., Rivera, A., LiPuma, L., Gallegos, A., Shi, C., Mack, M., and Pamer, E.G. (2009). Inflammatory monocytes facilitate adaptive CD4 T cell responses during respiratory fungal infection. *Cell Host Microbe* **6**, 470–481.
69. Wende, H., Lechner, S.G., Cheret, C., Bourane, S., Kolanczyk, M.E., Pattyn, A., Reuter, K., Munier, F.L., Carroll, P., Lewin, G.R., et al. (2012). The transcription factor c-Maf controls touch receptor development and function. *Science* **335**, 1373–1376.
70. Atarashi, K., Nishimura, J., Shima, T., Umesaki, Y., Yamamoto, M., Onoue, M., Yagita, H., Ishii, N., Evans, R., Honda, K., et al. (2008). ATP drives lamina propria T(H)17 cell differentiation. *Nature* **455**, 808–812.
71. Barman, M., Unold, D., Shifley, K., Amir, E., Hung, K., Bos, N., and Salzman, N. (2008). Enteric salmonellosis disrupts the microbial ecology of the murine gastrointestinal tract. *Infect. Immun.* **76**, 907–915.
72. DeTomaso, D., Jones, M.G., Subramaniam, M., Ashuach, T., Ye, C.J., and Yosef, N. (2019). Functional interpretation of single cell similarity maps. *Nat. Commun.* **10**, 4376.
73. Delaney, C., Schnell, A., Cammarata, L.V., Yao-Smith, A., Regev, A., Kuchroo, V.K., and Singer, M. (2019). Combinatorial prediction of marker panels from single-cell transcriptomic data. *Mol. Syst. Biol.* **15**, e9005.
74. Street, K., Rizzo, D., Fletcher, R.B., Das, D., Ngai, J., Yosef, N., Purdom, E., and Dudoit, S. (2018). Slingshot: cell lineage and pseudotime inference for single-cell transcriptomics. *BMC Genomics* **19**, 477.

STAR★METHODS

KEY RESOURCES TABLE

REAGENT or RESOURCE	SOURCE	IDENTIFIER
Antibodies		
Rat anti-mouse CD4 antibody, RM4-5, BUV737	BD	Cat#612844
TCR beta monoclonal antibody, H57-597, APC-eFluor780	eBioscience	Cat#47-5961-82
Anti-mouse CD45.1, A20, PerCP-Cyanine5.5	Tonbo	Cat#50-210-3580
Mouse anti-mouse CD45.2, 104, BV421	BD	Cat#562895
Anti-Human/Mouse CD45R (B220), RA3-6B2, PerCP-Cyanine5.5	Tonbo	Cat#65-0452-U100
CD103 Monoclonal antibody, 2E7, PE	eBioscience	Cat#12-1031-82
CD11b Monoclonal antibody, M1/70, APC-Cyanine7	Invitrogen	Cat#A15390
CD11c Monoclonal antibody, N418, PE-Cyanine7	eBioscience	Cat#25-0114-82
Anti-mouse CD24 antibody, M1/69, BV510	BioLegend	Cat#101831
CD62L Monoclonal antibody, MEL-14, FITC	eBioscience	Cat#11-0621-82
Anti-mouse CD64, X54-5/7.1, APC	BioLegend	Cat#139334
Anti-mouse CD69, H1.2F3, PE-Cyanine7	Tonbo	Cat#60-0691-U025
CD127 monoclonal antibody, A7R34, PE	eBioscience	Cat#12-1271-82
CD223 monoclonal antibody, eBioC9B7W, PerCP-eFluor710	eBioscience	Cat#46-2231-82
Rat monoclonal anti mouse MHCII, M5/114.15.2, Alexa Fluor 710	Tonbo	Cat#80-5321-U100
American Hamster monoclonal anti-g δ TCR, GL-3, GL3 APC	eBioscience	Cat#17-5711-82
CD366 monoclonal antibody, F38-2E2, APC	eBioscience	Cat#17-3109-42
Mouse monoclonal anti FoxP3, FJK-16s, BV421	eBioscience	Cat#404-5773-82
Fixable Viability Dye eFluor 506 (FVD)	Invitrogen	Cat#65-0866-14
Rat monoclonal anti- mouse IFN γ , XMG1.2, APC	eBioscience	Cat#17-7311-82
Rat monoclonal anti-mouse IL-17A, eBio17B7, FITC	eBioscience	Cat#11-7177-81
Goat monoclonal anti IL-22 antibody (POLY5164)	Biolegend	Cat#516406
Anti-mouse TIGIT, 1G9, BV421	BD	Cat#565270
Anti-mouse CD152, UC10-4F10-11, PE-Cyanine7	Tonbo	Cat#60-1522-U025
Anti-Human/Mouse CD44, IM7, APC	Tonbo	Cat#50-210-2735
Rat monoclonal anti-mouse NKp46, 29A1.4, PerCP-Cyanine5.5	eBioscience	Cat#46-3351-80
Rat monoclonal anti- mouse ROR γ t, PE	eBioscience	Cat#12-6988-82
c-MAF monoclonal antibody, sym0F1, PE	eBioscience	Cat#12-9855-42
Rat Anti-mouse GM-CSF, MP1-22E9, BV421	BD	Cat#564747
TCF1/TCF7 Rabbit mAb, C63D9, APC	Cell Signaling Technology	Cat#37636
Rat monoclonal anti-V β 14 TCR, 14-2(RUO), Biotin	BD Bioscience	Cat#553257
Rat Anti-mouse vb 14 T-Cell receptor, 14-2, FITC	BD	Cat#553258
Rat monoclonal anti- mouse ROR γ t, PE	eBioscience	Cat#12-6988-82
Anti-Rat CD196 (CCR6), 140706, BV421	BD Bioscience	Cat#564736
GATA3 Mouse, L50-823, BUV395	BD Bioscience	Cat#BDB565448
CD8a Monoclonal Antibody, 53-6.7, PE	eBioscience	Cat#12-0081-82
TotalSeq-B0301 anti-mouse Hashtag 1 Antibody	BioLegend	Cat#155831
TotalSeq-B0302 anti-mouse Hashtag 2 Antibody	BioLegend	Cat#155833

(Continued on next page)

Continued

REAGENT or RESOURCE	SOURCE	IDENTIFIER
TotalSeq-B0302 anti-mouse Hashtag 3 Antibody	BioLegend	Cat#155835
CD4 MicroBeads, mouse	Miltenyi Biotec	Cat#130-117-043
Bacterial strains		
<i>Segmented Filamentous Bacteria</i> (SFB)	K. Honda, Keio U	Umesaki et al. ⁶³
<i>Citrobacter rodentium</i>	D. Mucida, Rockefeller U	Esterházy et al. ⁶⁴
<i>Bifidobacterium adolescentis</i>	H. Wang, Columbia U	Huang et al. ⁶⁵
<i>Escherichia coli</i> Nissle 1917	M. Sommer, TU Denmark	Vaaben et al. ⁶⁶
Chemicals, peptides, and recombinant proteins		
In VivoMAb anti-mouse IL-10R antibody (clone 1B1.3A)	BioXcell	Cat#BE0050
CD3e monoclonal antibody, functional grade (clone 2C11)	eBioscience	Cat#16-0031-82
CD28 monoclonal antibody, functional grade (clone 37.51)	eBioscience	Cat#16-0281-38
Mouse anti-CTLA-4 Antibody (clone 63828)	R&D Systems	Cat#MAB434-100
InVivoMAb anti-mouse LAG-3 (clone C9B7W)	BioXcell	Cat#BE0174
InVivoMAB rat IgG1 isotype control (clone HRPN)	BioXcell	Cat#BE0088
Recombinant Mouse IL-23 Protein	R&D Systems	Cat#1887-ML
Recombinant Murine IL-1 β	PeptoTech	Cat#211-11B
Corning Dispase, 100 mL	Corning (Fisher)	Cat#354235
Roche Collagenase D 2.5g from <i>C.histoliticum</i>	Roche (Sigma)	Cat#11088882001
Collagenase, type 1, powder	Gibco	Cat#17018209
DeoxyribonucleaseI from bovine pancreas, 1g	Sigma	Cat#DN-25
Hanks' Balanced Salt solution (HBSS), 10X	CORNING	Cat#36320020
HyClone™ RPMI 1640 Medium, Sterile, pH 7.0 - 7.4, With L-glutamine, Liquid	Cytiva	CatSH30028.LS
Penicillin-Streptomycin (5.000U/ml)	Gibco	Cat#15070063
β -mercaptoethanol	Sigma-Aldrich	Cat#60-24-2
Sodium pyruvate (100 mM)	Gibco	Cat#11360070
L-Glutamin (200 mM)	Gibco	Cat#A2916801
MEM Non-Essential Amino Acids (100X)	Gibco	Cat#11140068
Sodium Bicarbonate	SIGMA	Cat#46H02825
Percoll®, Sterile, pH 8.5 - 9.5, Liquid	Cytiva	Cat#17-0891-09
Fetal Bovine Serum, Qualified, USDA approved	Thermo Scientific	Cat#10437028
HEPES(1M)	ThermoFisher	Cat#15630-080
Phenol/Chloroform/Isoamyl alcohol (25:24:1), stabilized	Fisher Scientific	Cat#327115000
Ambion TRIzol reagent	Fisher Scientific	Cat#15-596-018
2-Propanol, ACS reagent, $\geq 99.5\%$	Sigma-Aldrich	Cat#190764
Proteinase K	Lucigen	Cat#MPRK092
Cell Trace Violet cell proliferation kit	Life Technologies	Cat#34557
Ionomycin calcium salt from <i>Streptomyces</i>	Sigma-Aldrich	Cat#10634
PMA, for use in molecular biology	Sigma-Aldrich	Cat#P1585
Brefeldin A, from <i>Penicillium brefeldianum</i> , $\geq 99\%$ (HPLC and TLC)	Sigma Aldrich	Cat#B7651-5MG
Foxp3 / Transcription Factor Fix/Perm Concentrate (4X)	TONBO Biosciences	Cat#TNB-1020-L050
Foxp3 / Transcription Factor Staining Buffer Kit	TONBO Biosciences	Cat#TNB-0607-KIT

(Continued on next page)

Continued

REAGENT or RESOURCE	SOURCE	IDENTIFIER
Flow Cytometry Perm Buffer (10X)	TONBO Biosciences	Cat#TNB-1213-L150
Reinforced Clostridia Medium (RCM)	ThermoFisher	Cat#CM0149
LB Broth	Gibco	Cat#10855001

Critical commercial assays

Qscript cDNA Super Mix, QuantaBio	VWR	Cat#101414-108
2X Universal SYBR Green Fast qPCR Mix - 25 mL	ABclonal	Cat#RK21203
IFN gamma Mouse ELISA Kit	Invitrogen	Cat#BMS606-2
Lipocalin-2 (LCN2) Mouse ELISA Kit	Invitrogen	Cat#EMLCN2
cOMplete, EDTA-free protease-inhibitor	Roche	Cat#11836170001

Deposited data

Bulk RNA-seq intestinal Th17 cells	This Study	Bioproject: PRJNA1020879
Bulk RNA-seq TCF1 ⁺ and TCF1 ⁻ Th17 cells	This Study	Bioproject: PRJNA1020879
scRNA-seq SFB SI Th17 cells	This study	Bioproject: PRJNA1020879
scRNA-seq SFB SI Th17 cells WT and <i>Maf</i> ^{dIl17}	This study	Bioproject: PRJNA1020879
<i>In vitro</i> pathogenic vs. non-pathogenic Th17	Gaublomme et al. ¹³	GSE74833
Human IL-10 ⁻ Th17 vs. IL-10 ⁺ Th17	Aschenbrenner et al. ²⁹	GSE101389
CNS EAE Th17 vs. aCD3 SI IL-10 ⁺ Th17	Esplugues et al. ¹²	
c-MAF target genes	Ciofani et al. ³⁶	GSE40918
Exhausted CD4 T cells vs. effector CD4 T cells	Crawford et al. ²⁶	GSE41870

Experimental models: Organisms/strains

C57BL/6J, Room RB15	The Jackson Laboratory	Cat#000664
Ptprc (CD45.1)	The Jackson Laboratory	Cat#002014
<i>Cd4</i> ^{CRE}	The Jackson Laboratory	Cat#022071
7B8 TCR Tg	The Jackson Laboratory	Cat#027230
Rag1 ^{-/-}	The Jackson Laboratory	Cat#002216
<i>Il17a</i> ^{GFP}	The Jackson Laboratory	Cat#018472
<i>Il10</i> ^{-/-}	The Jackson Laboratory	Cat#002251
<i>Il10rb</i> ^{-/-}	The Jackson Laboratory	Cat#005027
<i>Foxp3</i> ^{mRFP}	The Jackson Laboratory	Cat#008374
<i>Il10</i> ^{GFP}	The Jackson Laboratory	Cat#008379
<i>Rosa26</i> ^{YFP}	The Jackson Laboratory	Cat#038215
<i>Il17a</i> ^{Katushka}	S. Huber, UKE	Gagliani et al. ²²
<i>Il10</i> ^{flox}	A. Roers, TU Berlin	Roers et al. ⁶⁷
<i>Il10</i> ^{Venus}	K. Honda, Keio U	Atarashi et al. ⁴
<i>Ccr2</i> ^{DTR}	E. Pamer, MSKCC	Hohl et al. ⁶⁸
<i>Maf</i> ^{flox}	N. Gagliani, UKE	Wende et al. ⁶⁹
<i>Tcf7</i> ^{mCherry}	This Study	N/A

Oligonucleotides

Il10 Fwd 5'-TTGGGTTGCCAAGCCTTATCG-3'	This Study	N/A
Il10 Rev 5'-AATCGATGACAGCGCCTCAG-3'	This Study	N/A
Maf Fwd 5'-GCGAAAGGGACGCCTACAAG-3'	This Study	N/A
Maf Rev 5'-AACAAGGTGGCTAGCTGGGA-3'	This Study	N/A
Il10rb Fwd 5'-TCAGTGCAGCTTCTCTCATCTTTC-3'	This Study	N/A
Il10rb Rev 5'-AGGAGGTCCAATGATGGTGTCTT-3'	This Study	N/A
Areg Fwd 5'-TACTTTGGTGAACGGTGTGGAG-3'	This Study	N/A
Areg Rev 5'-GCGAGGATGATGGCAGAGAC-3'	This Study	N/A
Tox Fwd 5'-GTGTGAGGATGCCTCCAAGATCAA-3'	This Study	N/A

(Continued on next page)

Continued

REAGENT or RESOURCE	SOURCE	IDENTIFIER
Tox Rev 5'-ACAAAGCATAGGCAGACACAGG-3'	This Study	N/A
Tcf7 Fwd 5'-GCGCGGGATAACTACGGAAA-3'	This Study	N/A
Tcf7 Rev 5'-GCCTAGAGCACTGTCATCGG-3'	This Study	N/A
Gzma Fwd 5'-GACACGGTTGTTCCCTCACTCA-3'	This Study	N/A
Gzma Rev 5'-CAATCAAAGCGCCAGCACAG-3'	This Study	N/A
Ccl5 Fwd 5'-TGCTGCTTTGCCCTACCTCTC-3'	This Study	N/A
Ccl5 Rev 5'-CCTTCGAGTGACAAACACGACT-3'	This Study	N/A
<i>Ifng</i> F 5'-CACGGCACAGTCATTGAAAG-3'	Kawano et al. ⁵⁷	N/A
<i>Ifng</i> R 5'-GCTGATGGCCTGATTGCTT-3'	Kawano et al. ⁵⁷	N/A
<i>Gapdh</i> F 5'-CCTCGTCCCGTAGACAAAATG-3'	Atarashi et al. ⁷⁰	N/A
<i>Gapdh</i> R 5'-TCTCCACTTTGCCACTGCAA-3'	Atarashi et al. ⁷⁰	N/A
SFB F 5'-GACGCTGAGGCATGAGAGCAT-3'	Barman et al. ⁷¹	N/A
SFB R 5'-GACGGCACGGATTGTTATTCA-3'	Barman et al. ⁷¹	N/A
UNI F 5'-ACTCCTACGGGAGGCAGCAGT-3'	Barman et al. ⁷¹	N/A
UNI R 5'-ATTACGCGGCTGCTGGC-3'	Barman et al. ⁷¹	N/A

Software and algorithms

Flow jo_v10.6.2	BD	N/A
Bowtie2 v2.3.4	N/A	N/A
10X Genomics Cellranger toolkit v1.0.1	N/A	N/A
USEARCH v11.0.667	N/A	N/A
GraphPad Prism version 9.1	N/A	N/A

Other

BD LSR Fortessa Flow Cytometer	BD	N/A
BD Aria, Floy Cytometer	BD	N/A
Irradiated Normal Chow Diet, Lab diet 5061 (NCD, Pico-Vac Rodent Diet 20)	Lab Diet	Cat#5061
Zirconia/Silica Beads 0.1mm	Fisher Scientific	Cat#11079101z
Miltenyi Biotec, Inc. LS Columns 25/PK	Miltenyi Biotec	Cat#130-042-401
LightCycler® 480 System	Roche	N/A
Fisherbrand Razor Blades	Fisher Scientific	Cat#12640
Insulin Syringes with Permanently Attached Needles	BD	Cat#329420
Cell Strainer, Individual Package, 40 um, blue	VWR	Cat#76327-098
Bead beater	Biospec	Cat#1001
Beads cleanup	Beckman Coulter	Cat#A63881

RESOURCE AVAILABILITY

Lead contact

Further information and requests for resources and reagents should be directed to and will be fulfilled by the lead contact, Ivaylo Ivanov (ii2137@cumc.columbia.edu).

Materials availability

Mouse lines generated in this study are available upon request from the [lead contact](#) under an institutional MTA.

Data and code availability

- Sequencing data have been deposited at NCBI BioProject database (<http://www.ncbi.nlm.nih.gov/bioproject/>) and are publicly available as of the date of publication. Accession numbers are listed in the [key resources table](#).
- This paper does not report original code. References to all code used are available in the [STAR Methods](#) section.
- Any additional information required to reanalyze the data reported in this paper is available from the [lead contact](#) upon request.

EXPERIMENTAL MODEL AND STUDY PARTICIPANT DETAILS

In vivo animal studies

Mice

C57BL/6J, Ly5.1 (CD45.1), RAG1-deficient, *Il17a^{GFP}*, *Il17a^{Cre}*, *Il10^{GFP}*, *Foxp3^{mRFP}*, *Il10^{-/-}*, *Il10rb^{-/-}* and 7B8 transgenic mice were purchased from the Jackson Laboratory. Animals were purchased only from SFB-negative maximum barrier rooms. All animals were tested for SFB upon arrival and maintained in an SFB-negative high barrier room at Columbia University. 7B8 mice were bred to Ly5.1 and *Il17a^{GFP}* mice at Columbia University. *Il17a^{Katushka}* mice²² were provided by Dr. Samuel Huber, University Medical Center Hamburg-Eppendorf (UKE) with permission from Dr. Richard Flavell, Yale and bred at Columbia University. 7B8 mice were bred to Ly5.1 and to *Il10^{GFP}*, *Il17a^{Katushka}*, *Foxp3^{mRFP}* mice at Columbia University. *Maif^{fl/fl}* mice⁶⁹ on C57BL/6 background were obtained from Dr. Nicola Gagliani, UKE and Dr. Arnold Han, Columbia University with permission from Dr. Carmen Birchmeier, Max Delbrück Center for Molecular Medicine (MDC) and bred at Columbia University. *Ccr2^{DTR}* mice⁶⁸ were gifted by Dr. Eric Pamer, Memorial Sloan-Kettering Cancer Center. *Il10^{lox}* mice⁶⁷ were obtained from Dr. A. Roers, Technische Universität Dresden and bred to *Cd4^{Cre}* mice at Columbia University. *Il10^{Venus}* mice⁴ were gifted by Dr. Kenya Honda, Keio University with permission from Dr. Kiyoshi Takeda, Osaka University and bred to *Tcf7^{mCherry}* mice at Columbia University. *Tcf7^{mCherry}* mice on C57BL/6 background were generated using CRISPR/Cas9 based gene editing. The targeted vector contains an mCherry reporter sequence preceded by a splice acceptor site and a P2A self-cleaving sequence placed in intron 2 and surrounded by a pair of non-complementary *LoxP* sites (Figure S5). The targeting construct also contained an inversion of the *Tcf7* genomic sequence containing Exons 3-4 surrounded by two pairs of *LoxP* and *LoxP2272* sequences in opposite orientation in intron 2 and intron 5. The targeted reporter allele therefore expresses mCherry and is a functional knock-out for TCF1 that can be conditionally activated upon expression of Cre-recombinase (Figure S5). All animals used in this study were *Tcf7^{mCherry/+}* and therefore heterozygous for *Tcf7*. All mouse strains were bred and housed under specific pathogen-free conditions at Columbia University Medical Center under IACUC approved guidelines. To control for microbiota and cage effects, experiments were performed with gender matched littermate control animals that were housed in the same cage.

Bacterial colonization and infection

SFB colonization was performed by single oral gavage of fecal suspension from SFB-enriched mice as previously described.⁴² To control for variability in SFB levels in feces used for gavage, all gavages were performed with frozen stocks from a single batch of SFB-enriched feces. Fecal samples were tested for SFB by quantitative RT-PCR and frozen as batch aliquots at -80C. Control SFB-negative feces were collected in a similar manner. SFB colonization levels were confirmed by qPCR and normalized to levels of total bacteria (UNI) as previously described.⁴²

Bifidobacterium adolescentis (*Ba*) and *Escherichia coli* (*Ec*) were gavaged at 10⁸ CFU/animal every other day for 14 days. *Ba* was grown in Reinforced Clostridial Medium in an anaerobic chamber (5% H₂, 10% CO₂, 85% N₂) at 37C for 48 hours. *Ec* was grown overnight in Luria-Bertani (LB) broth at 37C.

For *Citrobacter rodentium* infections, mice were infected with 1 x 10⁹ CFU by oral gavage.

Transfer colitis

FACS-sorted CD45RB^{high} CD4⁺ T cells from spleen and lymph nodes were injected i.v. (5x10⁵ cells/mouse) into RAG1-deficient mice. Lipocalin-2 in fecal samples was measured by ELISA.

In vivo suppression assay

Naïve 7B8 CD4⁺ T cells were isolated from spleen of 7B8.Ly5.1 *Il17a^{GFP}* transgenic mice (Ly5.1) by FACS (Ly5.1⁺Vβ14⁺CD4⁺TCRβ⁺CD62L⁺CD44^{neg}CD25^{neg}). Intestinal SFB Th17 cells (CD4⁺TCRβ⁺IL-17^{GFP+}) and Foxp3⁺ Treg (CD4⁺TCRβ⁺Foxp3^{mRFP+}IL-17^{Katushka-}) cells were isolated from SI LP of *Il17a^{GFP}* or *Foxp3^{mRFP}* Ly5.2 mice respectively by FACS two weeks after SFB colonization. 30,000 naïve 7B8 CD4⁺ T cells and 30,000 SI LP cells were injected intravenously in a 1:1 ratio into SFB-colonized Rag1^{-/-} mice. Expansion and Th17 cell differentiation of Ly5.1⁺ 7B8 CD4⁺ T cells was analyzed in SI LP and mLN on day 8 post transfer. To assess the role of IL-10 signaling, anti-IL-10R antibody (200 μg/mouse clone 1B13A, Bio X Cell) or an isotype control antibody were injected on day 2, 4 and 6 post transfer.

Adoptive transfers

SFB-negative WT, *Il10^{-/-}*, *Il10rb^{-/-}*, or *Il10^{ΔT}* mice were gavaged with SFB-containing fecal pellets as described above. Five days after gavage, MACS-purified (CD4 beads, Miltenyi) 7B8 or total CD4⁺ T cells from spleen and LN of SFB-negative (naïve) 7B8.Ly5.1 *Il10^{eGFP}*/*Il17a^{Katushka}*/*Foxp3^{mRFP}* or Ly5.1 *Il10^{eGFP}*/*Il17a^{Katushka}*/*Foxp3^{mRFP}* mice were transferred intravenously (5x10⁵ 7B8 cells/recipient or 2x10⁶ total CD4⁺ T cells/recipient).

Migration assays

Il17a^{GFP} reporter mice or *Tcf7^{mCherry}*/*Il17a^{GFP}* double reporter mice were gavaged with SFB-containing feces as described above. Two weeks after gavage, SI LP lymphocytes were isolated and SFB Th17 cells (Ly5.1⁺CD4⁺TCRβ⁺IL-17^{GFP+}) or TCF1⁺ SFB Th17 cells (Ly5.1⁺CD4⁺TCRβ⁺IL-17^{GFP+}TCF1^{mCherry+}) were FACS-purified. 50,000 SI LP Th17 cells (combined from multiple mice) were

injected intravenously into SFB-colonized WT mice (Ly5.2). Cells were isolated from mLN, LI LP, SI LP and liver at indicated time-points to examine transferred Ly5.1⁺ CD4⁺ T cell.

Mixed bone marrow chimeras

Total bone marrow cells were isolated from *Ccr2*^{DTR} mice, *Il10rb*^{-/-} and WT C57BL/6 mice (all Ly5.2). After removal of red blood cells, *Ccr2*^{DTR} bone marrow cells were mixed in a 1:1 ratio with *Il10rb*^{-/-} or WT bone marrow cells and five million total cells were transferred into lethally irradiated (11 Grey) recipient WT Ly5.1 mice. 12 weeks later, mice were colonized with SFB as described above. The mice were treated with 20 ng/g diphtheria toxin (DT) every other day starting on Day -1. Ly5.1/Ly5.2 7B8 triple reporter CD4⁺ T cells were transferred on Day 0 as described earlier. Th17 cell differentiation in SI LP was analyzed on Day 7. For Q-PCR analysis, intestinal cells were FACS-purified and sorted into TRIZOL reagent (Life technology).

METHOD DETAILS

In vitro suppression assay

Responder naïve CD4⁺ T cells (WT or *Il10rb*^{-/-}) isolated from spleen were purified via FACS (CD4⁺TCRβ⁺CD62⁺CD44⁻CD25⁻). Responder CD4⁺ T cells were labeled with 5 μM CellTrace violet dye (proliferation dye, Invitrogen) and stimulated in the presence of irradiated splenic APCs (25 Grey) and 1 μg/ml soluble anti-CD3 (clone 2C11). Responder CD4⁺ T cells were cultured in the absence or presence of indicated SI LP CD4⁺ T cells in a 2:1 ratio for 4 days. SFB and *Crod* Th17 cells (CD4⁺TCRβ⁺IL-17^{GFP+}) were isolated from SI LP or LI LP of *Il17a*^{GFP} reporter mice two weeks after SFB gavage or *Crod* infection respectively. Foxp3⁺ Treg cells were isolated from SI LP of *Foxp3*^{mRFP} reporter mice. To assess the role of IL-10 signaling and co-inhibitory receptors, blocking antibodies against IL-10R, CTLA-4 or LAG-3 were added to some of the cell culture (anti-mouse IL-10R (1B1.3A), 10 μg/ml, Bio X Cell; anti-mouse CTLA-4 (63828), 10 μg/ml, R&D Systems; anti-mouse LAG-3 (C9B7W), 10 μg/ml, Bio X Cell). Division Index (DI) was calculated with FlowJo based on the divisions of responder T cells. Percent suppression was calculated using the following formula:

$$\% \text{ suppression} = 100 - 100 \times (\text{DI}(\text{responder} + \text{suppressor}) / \text{DI}(\text{responder alone}))$$

Lymphocyte isolation from intestine and flow cytometry

Lamina propria lymphocytes isolation from intestine was performed as previously described.⁴² In brief, Peyer's patched (SI) were removed and intestines were opened longitudinally. After washing, the intestines were cut into 1 cm long pieces and incubated in 5 mM EDTA solution twice for 20 min at 37°C. Lamina propria lymphocytes were isolated by digesting the tissue with Collagenase D, DNase and Dispase three times for 20 min at 37°C. Lymphocytes were further purified using 80:40 Percoll gradient. After isolation cells were analyzed immediately by flow cytometry. For intracellular cytokine and transcription factor staining, the cells were re-stimulated with PMA/Ionomycin for 3 hours in the presence of Brefeldin A, followed by fixation and permeabilization using Foxp3/transcription factor staining buffer kit (Tonbo) according to manufacturer protocol. Dead cells were excluded with fixable viability dye (eFluor506, Invitrogen).

In vitro culture

Tcf7^{mCherry}/*Il17a*^{GFP}/*Il10*^{Venus} triple reporter mice were gavaged with SFB-containing feces or infected with *Citrobacter rodentium* as described above. Lymphocytes were isolated two weeks later from terminal ileum (distal quarter of SI) or duodenum (proximal quarter of SI) (SFB-gavaged) or LI LP (*Crod*-infected). TCF1⁺ Th17 cells (CD4⁺TCRβ⁺IL-17^{GFP+}TCF1^{mCherry+}IL-10^{Venus-}) were FACS-purified from individual mice and plated in 96-well plates coated with 5 μg/ml aCD3 antibody (clone 2C11) in the presence of 5 μg/ml soluble aCD28 antibody (clone 37.51) for four days. Additionally, FACS-sorted SFB TCF1⁺ Th17 cells (CD4⁺TCRβ⁺IL-17^{GFP+}TCF1^{mCherry+}IL-10^{Venus-}) were plated in 96-well plates coated with 5 μg/ml aCD3 antibody (clone 2C11) in the presence of 5 μg/ml soluble aCD28 antibody (clone 37.51), 10 ng/ml IL-23 and 10 ng/ml IL-1β for four days.

Lipocalin-2 ELISA

Lipocalin-2 was measured in fecal pellets from colitogenic mice. Fecal pellets were weighed and disrupted in PBS containing cOmplete protease inhibitor (Roche). After centrifugation, supernatant was collected and stored in -80°C until Lipocalin-2 ELISA was performed. ELISA was performed according to manufacturer protocol.

IFN-γ ELISA

Cell culture supernatants were collected from *in vitro* cultures of SFB TCF1⁺ Th17 cells after four days in the presence or absence of IL-23 and IL-1β. IFN-γ ELISA was performed according to the manufacturer protocol.

Quantitative PCR

mRNA from FACS-sorted cells was isolated using TRIZOL reagent (Life technology) according to the manufacturer protocol. Reverse transcription was performed with QScript cDNA SuperMix (QuantaBio). Q-PCR was performed using SYBR Green on LightCycler 480 (Roche). Samples were analyzed using the ΔΔCt method and normalization to *Gapdh*.

Bulk RNA-sequencing and analysis

LP TCR β^+ CD4 $^+$ IL-17 $^{GFP^+}$ Th17 cells were purified via FACS from small or large intestine two weeks after gavage with SFB or infection with *Citrobacter rodentium*, or 10 weeks after colitis induction (CD45RB hi colitis). Total mRNA was isolated using TRIZOL (Life technology) as per the manufacturer protocol. RNA-sequencing (RNA-Seq) was performed at the JP Sulzberger Columbia Genome Center. RNA amplification and library preparation was performed using the CLONTECH kit by Takara Bio. Libraries were then sequenced using Illumina NovaSeq 6000 (~40M reads). RTA (Illumina) was used for base calling and bcl2fastq2 (version 2.20) for converting BCL to FASTQ format. Raw reads were then processed by Cutadapt v2.1 with the following parameters: '-minimum-length 30:30 -u 15 -u -5 -U 15 -U -5 -q 20 -max-n 0 -pair-filter=any' to remove low-quality bases and Illumina adapters. Next, pseudoalignment was performed against the index created from mouse transcriptomes (GRCm38) using Kallisto (0.44.0). Differential gene expression analysis was performed by DESeq2 using reads count estimated by pseudoalignment, and the sets of differentially expressed genes were identified using the following steps: First, genes that were not significantly changed were excluded (padj < 0.05). Next, genes with very low expression level (transcripts per million, TPM < 5 in at least 9 out of the 10 samples) were also excluded. Finally, an unusually high level of Ig gene transcripts was observed in a few samples and, therefore, Ig genes were excluded from the analysis.

Gene set enrichment analysis (GSEA)

To identify if curated signature gene sets or other specific gene sets are up-regulated or down-regulated compared to published datasets, we performed gene set enrichment analysis. Briefly, normalized gene expression levels by microarray or RNA-seq were obtained from NCBI Gene Expression Omnibus or the original publication. Next, fold-changes of gene expression between comparisons were calculated in R v.4.1.0, and normalized enrichment scores as well as p-values of given gene sets were then estimated using the fgsea R package v.1.24.0 with the setting "nperm=1000".

Identification of c-MAF target genes

To identify potential c-MAF target genes, we extracted results from a regulatory network analysis for Th17 cell³⁶ that integrated ChIP-seq data and RNA-seq data. Briefly, the summed scores for KC network of c-MAF were extracted from the original publication and genes with a score greater than 2 were defined as c-MAF target genes.

Single cell RNA-sequencing and analysis

SI LP SFB Th17 cells (TCR β^+ CD4 $^+$ Foxp3 mRFPneg IL-17 $^{Katushka^+}$) were FACS-sorted from SFB-colonized *Il10^{eGFP}/Il17a^{Katushka}/Foxp3^{mRFP}* mice. In a second set of experiments, Th17 cells (TCR β^+ CD4 $^+$ IL-17 $^{YFP^+}$) were FACS-sorted from SI LP of *Foxp3^{mRFP}/Il17a^{Cre}/Maf^{flox/flox}/R26^{STOP-YFP}* mice (*Maf^{ΔIL17}*) (n=2) and *Foxp3^{mRFP}/Il17a^{Cre}/Maf^{flox/+}/R26^{STOP-YFP}* (WT) mice (n=3) two weeks after SFB gavage. Prior to sorting, cells from individual animals were labelled using hashtag antibodies conjugated to nucleotide barcodes (BioLegend, #155831, #155833, #155835). scRNA-seq was performed at the JP Sulzberger Columbia Genome Center using the 10X Genomics platform with a target of 5,000 nuclei per sample and 130M reads. Next, reads alignment, filtering, and barcode counting were performed using Cell Ranger v.3.0.2. All single-cell analyses were performed using R v.4.1.0 and Python v.3.6. Briefly, Seurat v.4.0.5 was utilized for preprocessing, normalization, and clustering. Ggplots2 v.3.3.5 was used to generate UMAP and dot plots. Low quality cell profiles were excluded if they met one of the following criteria: (i) number of genes expressed 200 or 2500 or (ii) 5% of the total unique molecular identifiers (UMIs) were mitochondrial RNA. The data was then normalized using the NormalizeData function. Wild type and *Maf^{ΔIL17}* Th17 cells were integrated using the SCTransform and FindIntegrationMarkers. Next, the RunPCA function was applied followed by FindNeighbors and FindClusters functions on the number of PCs selected using the ElbowPlot function. Marker genes that were differentially expressed within each cluster were identified by the FindAllMarkers function with average log-transformed fold change cutoffs of 0.25 and pct cutoffs of 0.25. Gene set scoring was performed using the VISION R package v.3.0.0.⁷² Gene set enrichment scores and p-values were computed using the fgsea R package v.1.24.0, a fast algorithm for Gene Set Enrichment Analysis (GSEA). Genes were ranked utilizing the wilcoxauc function from the presto R package, which performs a Wilcoxon rank sum test. COMET Python package⁷³ was applied to predict cell surface markers for clusters of interest. COMPASS Python package⁴⁸ was applied to characterize cellular metabolic states for clusters of interest. Slingshot v.2.2.0⁷⁴ was used for trajectory analysis starting at the progenitor-like population (C4).

QUANTIFICATION AND STATISTICAL ANALYSIS

Statistical significance was determined by unpaired t test with Welch's correction or other methods as noted on figure legends. P values are represented on figures as follows: ns, not significant, * p < 0.05, ** p < 0.01, *** p < 0.005, **** p < 0.001, ***** p < 0.0005. Error bars on all figures represent standard error of the mean. Statistical analysis was performed using GraphPad Prism version 9.1 for Windows (GraphPad Software).

Immunity, Volume 56

Supplemental information

**Intestinal microbiota-specific Th17 cells
possess regulatory properties and suppress
effector T cells via c-MAF and IL-10**

Leonie Brockmann, Alexander Tran, Yiming Huang, Madeline Edwards, Carlotta Ronda, Harris H. Wang, and Ivaylo I. Ivanov

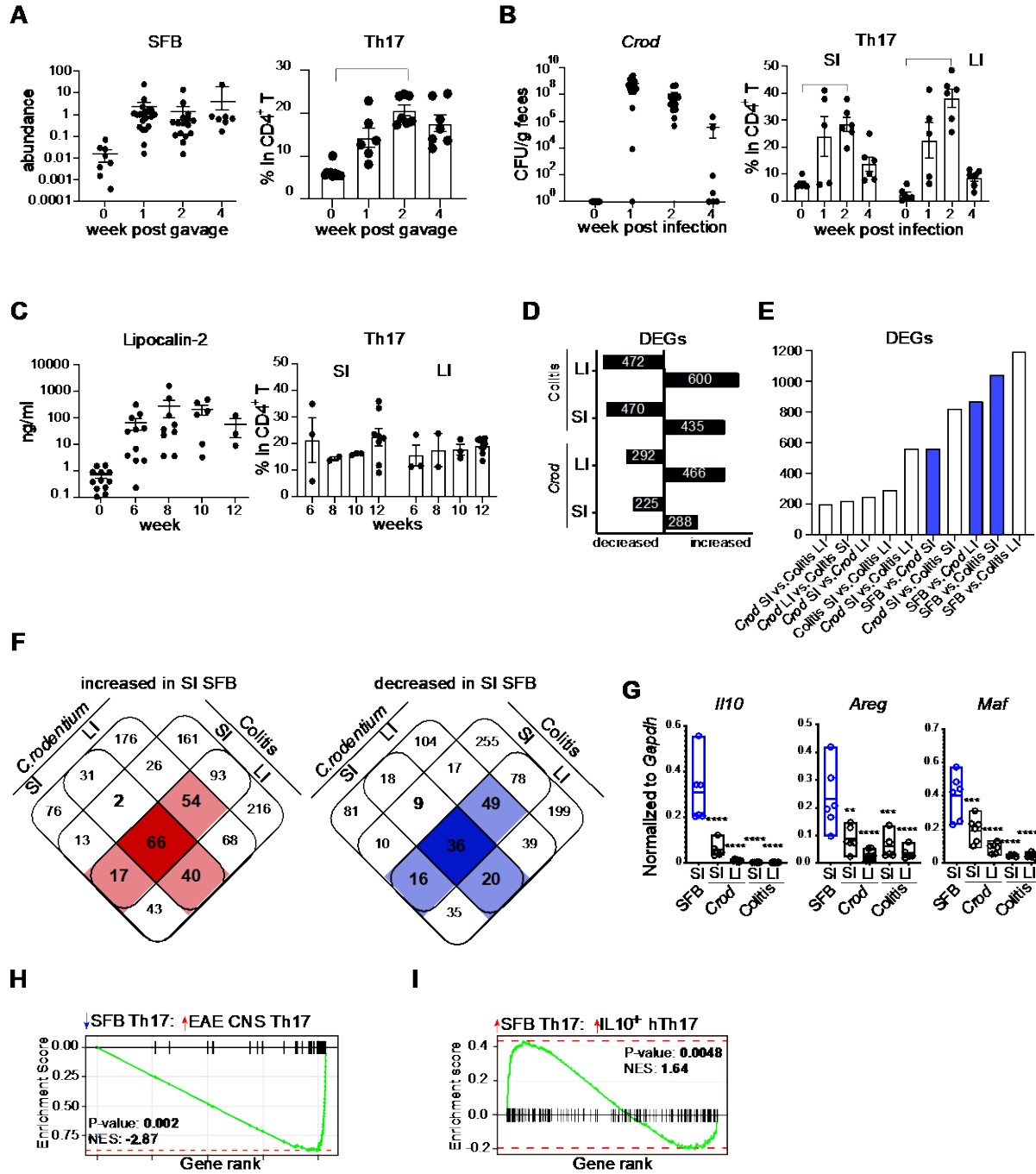


Figure S1. SFB Th17 cells are transcriptionally distinct from other intestinal Th17 cells. Related to Figure 1

(A) *Il17a^{GFP}* mice were colonized with SFB by oral gavage. (Left) Relative abundance of SFB 16S DNA in feces over time. (Right) Frequency of SI LP Th17 cells over time. Three independent experiments, n = 6-15 mice/timepoint.

(B) *Il17a^{GFP}* mice were infected with *Citrobacter rodentium* (*Crod*) (1×10^9 CFU/mouse) by oral gavage. (Left) Colony forming units (CFU)/g feces over time. (Right) Frequency of SI LP and LI LP Th17 cells over time. Three independent experiments, n = 5-10 mice/timepoint.

(C) Naive CD45RB^{hi} CD4⁺ T cells were purified from spleens of *Il17a^{GFP}* mice and adoptively transferred into RAG1-deficient recipients. (Left) ELISA for Lipocalin-2 in fecal samples over time. (Right) Frequency of SI LP and LI LP Th17 cells over time. One experiment, n = 3-7 mice/timepoint.

(D) Number of differentially expressed genes (DEGs) in bulk RNA-Seq samples of SI LP SFB Th17 cells compared to other intestinal Th17 cells.

(E) Number of DEGs in each pairwise comparison between various intestinal Th17 cells. Pairwise comparisons that include SFB Th17 cells are marked in blue.

(F) Venn Diagrams of DEGs in (D). (Left) Genes increased in SFB Th17 cells compared to other datasets. Genes increased in SFB Th17 cells compared to three (light red) or all four (dark red) datasets are colored. (Right) Genes decreased in SFB Th17 cells compared to other datasets. Light blue, decreased compared to three datasets. Dark blue, decreased compared to all four datasets.

(G) Quantitative PCR of *Il10*, *Areg* and *Maf* transcripts in FACS-purified intestinal Th17 cells. Two independent experiments, n = 5-6 mice/group.

(H) GSEA of genes decreased in SFB Th17 cells compared with genes increased in inflammatory Th17 cells.

(I) GSEA of genes increased in SFB Th17 cells compared to genes increased in human IL-10⁺ Th17 cells.

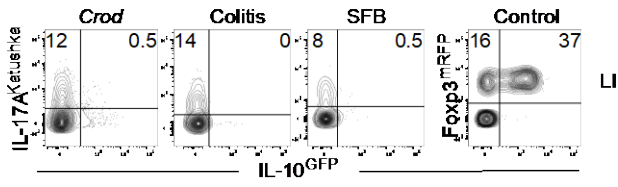
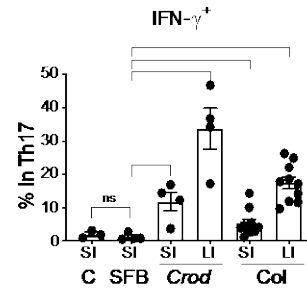
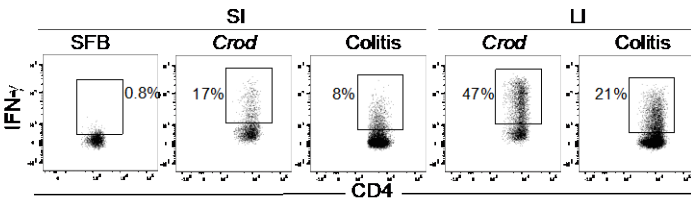
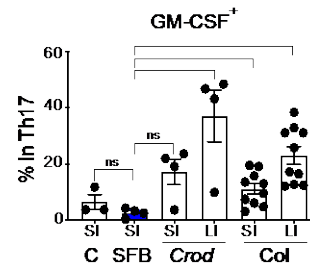
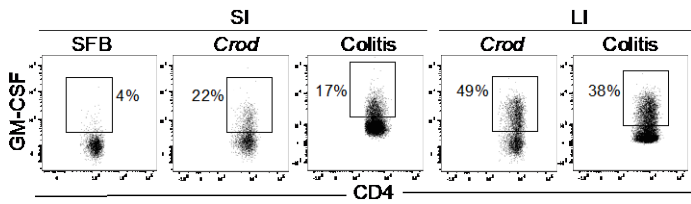
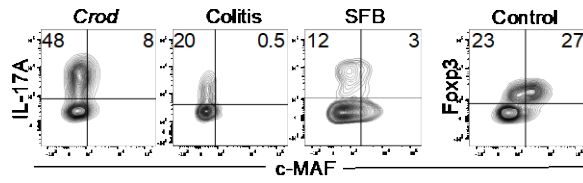
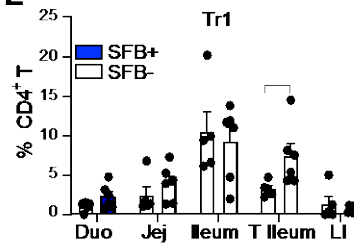
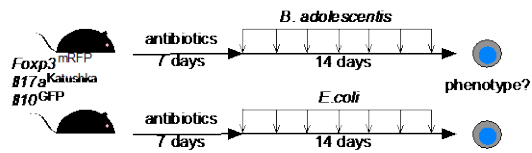
A**B****C****D****E****F**

Figure S2. SFB Th17 cells have a distinct cytokine expression profile. Related to Figure 2

Intestinal Th17 cells were induced by various methods (see text) in *Il10^{GFP}/Il17a^{Katushka}/Foxp3^{mRFP}* mice.

(A) IL-10^{GFP} expression in Th17 cells and Foxp3^{mRFP+} Treg cells from LI LP. Gated on TCRβ⁺CD4⁺Foxp3^{mRFPneg} LI LP lymphocytes (*Cod*, Colitis, SFB) or TCRβ⁺CD4⁺ LI LP lymphocytes (Control).

(B) IFN-γ expression in SI LP and LI LP Th17 cells. Plots gated on TCRβ⁺CD4⁺IL-17⁺ LP lymphocytes. Several independent experiments, n = 3-10 mice/group.

(C) GM-CSF expression in SI LP and LI LP Th17 cells. Plots gated on TCRβ⁺CD4⁺IL-17⁺ LP lymphocytes. Several independent experiments, n = 3-10 mice/group.

(D) c-MAF expression in LI LP Th17 cells and Foxp3⁺ Tregs. FACS plots gated on TCRβ⁺CD4⁺ lymphocytes.

(E) Frequency of Tr1 cells (CD4⁺TCRβ⁺Foxp3^{mRFP}-IL-17^{Katushka}-IL-10^{GFP+}) in indicated parts of the intestine before and two weeks after colonization with SFB. Four independent experiments, n = 5-6 mice/group.

(F) Experimental scheme of oral gavage of *Il10^{GFP}/Il17a^{Katushka}/Foxp3^{mRFP}* mice with *Bifidobacterium adolescentis* or *E. coli*.

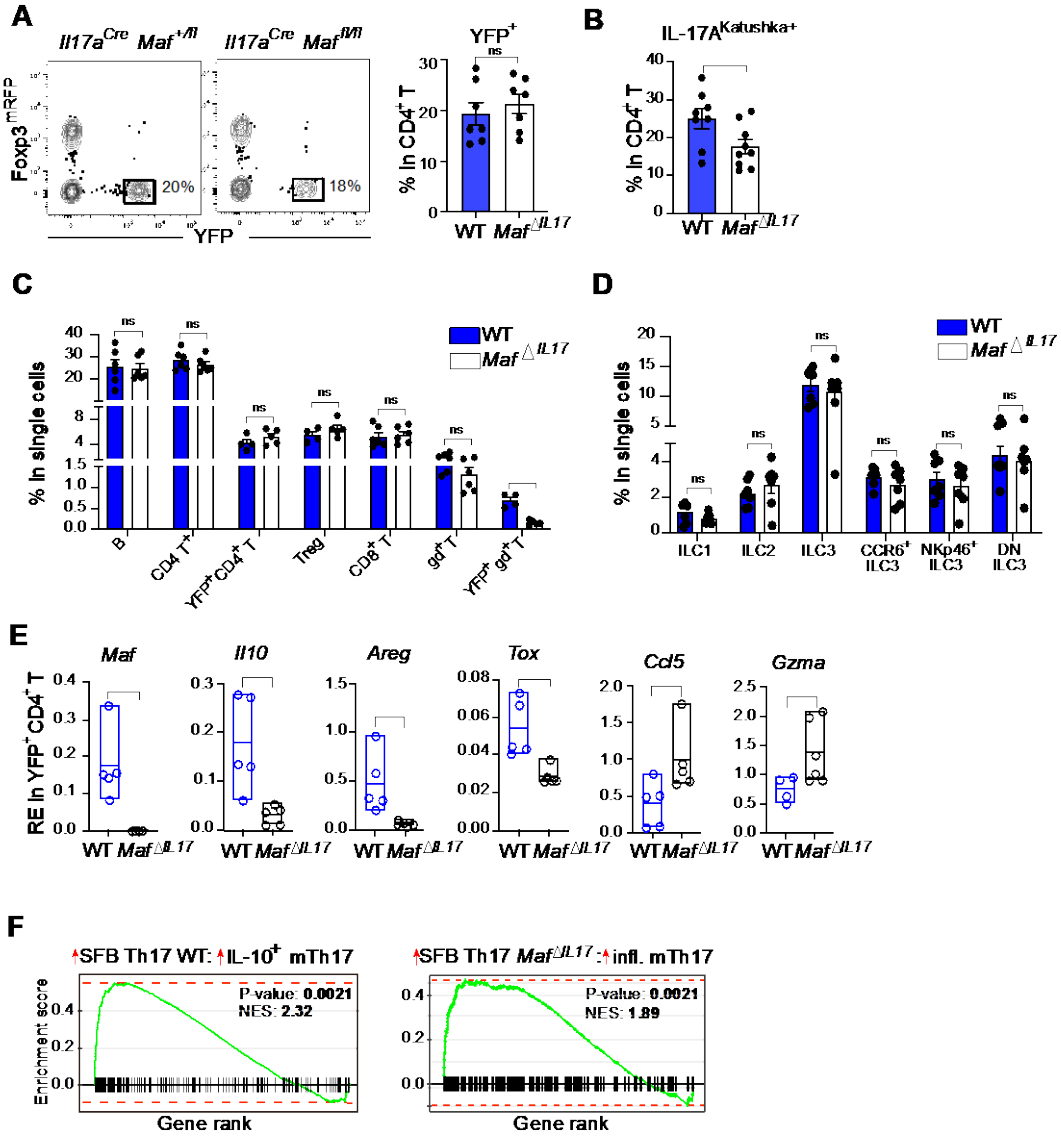


Figure S3. c-MAF drives anti-inflammatory identity of commensal Th17 cells.

Related to Figure 3

(A) Foxp3^{mRFP} and ROSA^{YFP} expression in SI LP CD4⁺ T cells in *Foxp3^{mRFP}/R26^{STOP-YFP}/Il17a^{Cre}/Maf^{flox/flox}* (*Maf^{ΔIL17}*) mice and *Foxp3^{mRFP}/R26^{STOP-YFP}/Il17a^{Cre}/Maf^{flox/+}* (WT) littermates. (Left) Representative FACS plots. (Right) Proportion of ROSA^{YFP+} (Th17) cells. Gated on CD4⁺ T cells (TCRβ⁺CD4⁺).

(B) Proportion of IL-17A^{Katushka+} Th17 cells in CD4⁺ T cells from SI LP of *Il10^{GFP}/Il17a^{Katushka}/Foxp3^{mRFP}/R26^{STOP-YFP}/Il17a^{Cre}/Maf^{flox/flox}* (*Maf^{ΔIL17}*) and littermate control (WT) mice.

(C) Frequency of adaptive immune cell subsets in SI LP of WT and *Maf^{ΔIL17}* mice. Two independent experiments, n = 6 mice/group

(D) Frequency of indicated ILC subsets and ILC3 subsets in SI LP of WT and *Maf^{ΔIL17}* mice. Two independent experiments, n = 6 mice/group

(E) Quantitative PCR for indicated genes in FACS-purified YFP⁺ SI LP Th17 cells from *Foxp3^{mRFP}/R26^{STOP-YFP}/Il17a^{Cre}/Maf^{flox/flox}* (*Maf^{ΔIL17}*) mice and WT littermates. Two independent experiments, n = 5 mice/group.

(F) (Left) GSEA of top 200 genes increased in YFP⁺ WT SI LP SFB Th17 cells compared to genes increased in mouse IL-10⁺ Th17 cells. (Right) GSEA of top 200 genes increased in YFP⁺ *Maf^{ΔIL17}* SI LP SFB Th17 cells compared to genes increased in inflammatory (CNS EAE) Th17 cells.

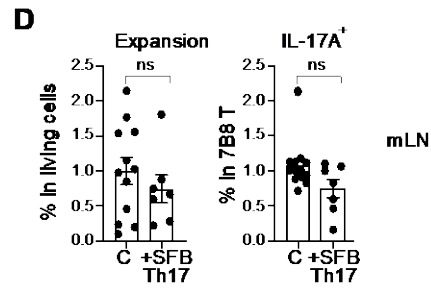
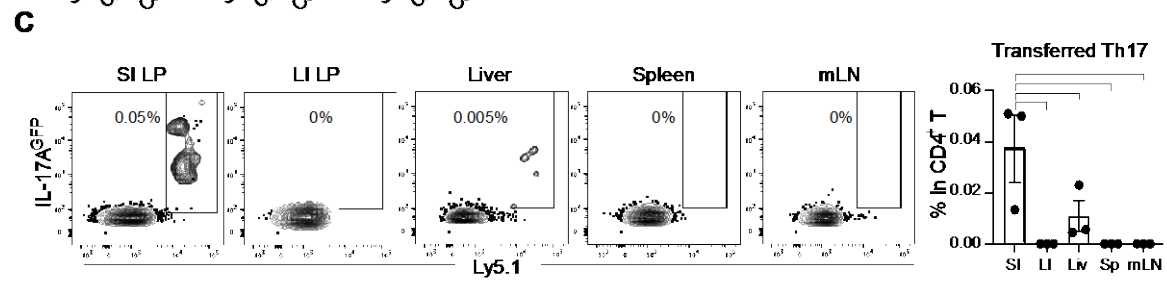
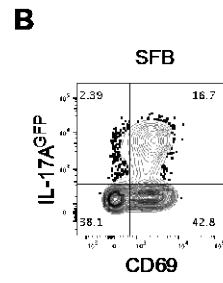
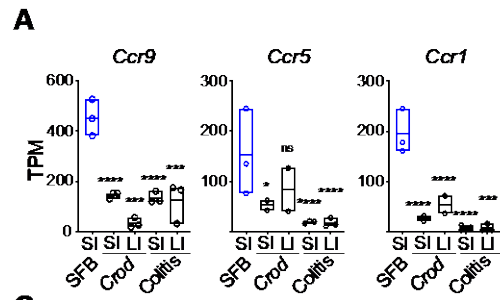


Figure S4. SFB Th17 cells have features of tissue resident T cells. Related to Figure 4

(A) Expression of select chemokine receptors in RNA-Seq samples from various intestinal LP Th17 cells in Figure 1B.

(B) Representative FACS plot of CD69 expression in SI LP SFB Th17 cells two weeks after SFB colonization of *Il17a^{GFP}* reporter mice.

(C) Th17 cells ($\text{TCR}\beta^+\text{CD4}^+\text{IL-17}^{\text{GFP}+}$) were FACS-purified from SI LP of SFB-colonized *Ly5.1/Il17a^{GFP}* reporter mice and adoptively transferred into WT congenic recipients. Representation and phenotype of transferred Ly5.1^+ cells were examined two days later in various tissues. Plots gated on $\text{TCR}\beta^+\text{CD4}^+$ (left) and $\text{TCR}\beta^+\text{CD4}^+\text{Ly5.1}^+$ (right). One experiment, $n = 3$ recipient mice.

(D) Expansion and Th17 cell differentiation of naive 7B8 CD4^+ T cells (Ly5.1) in mesenteric lymph nodes (mLN) 8 days after transfer into SFB-colonized RAG1-deficient mice alone (C) or with SI LP SFB Th17 cells. Cumulative of three independent experiments, $n = 7-12$ mice/group. Each datapoint was normalized to the average of the corresponding control (C) group within each experiment.

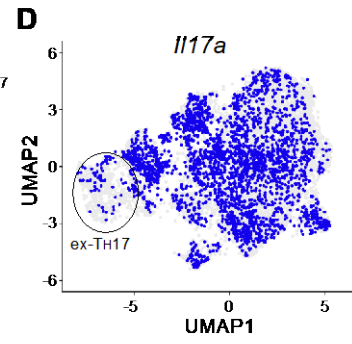
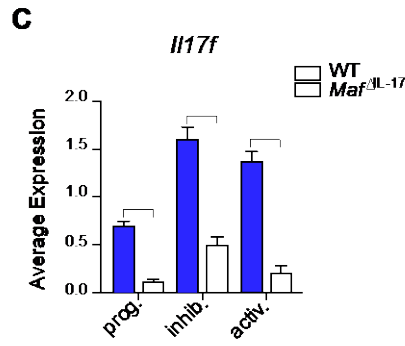
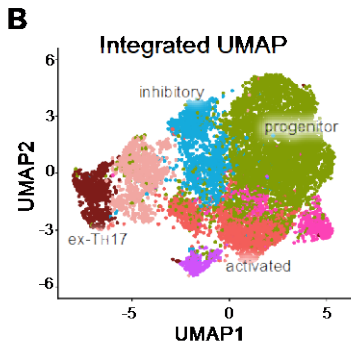
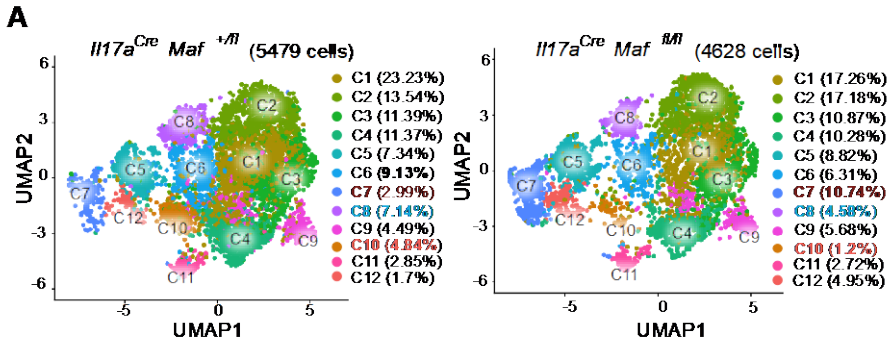


Figure S5. scRNA-Seq analysis of WT and $Maif^{ΔL17}$ Th17 cells. Related to Figure 5

(A) UMAP cluster annotation of scRNA-seq of FACS purified YFP⁺ SI LP SFB Th17 cells from $R26^{STOP-YFP}/I117a^{Cre}/Maif^{lox/+}$ and $R26^{STOP-YFP}/I117a^{Cre}/Maif^{lox/lox}$ mice. One experiment, n = 2-3 mice/group.

(B) Integrated UMAP of all 10,107 cells with functional annotation of the clusters in (A). One experiment, n = 2-3 mice/group.

(C) Expression of *I117f* mRNA in indicated functional groups in SI LP SFB YFP⁺ Th17 cells from WT (blue) and $Maif^{ΔL17}$ mice (white), based on hash-tagged samples from the scRNA-Seq experiment in (A).

(D) Expression of *I117a* in individual Th17 cells in the integrated UMAP of all cells from samples in (A). Cluster C7 represents ex-Th17 cells.

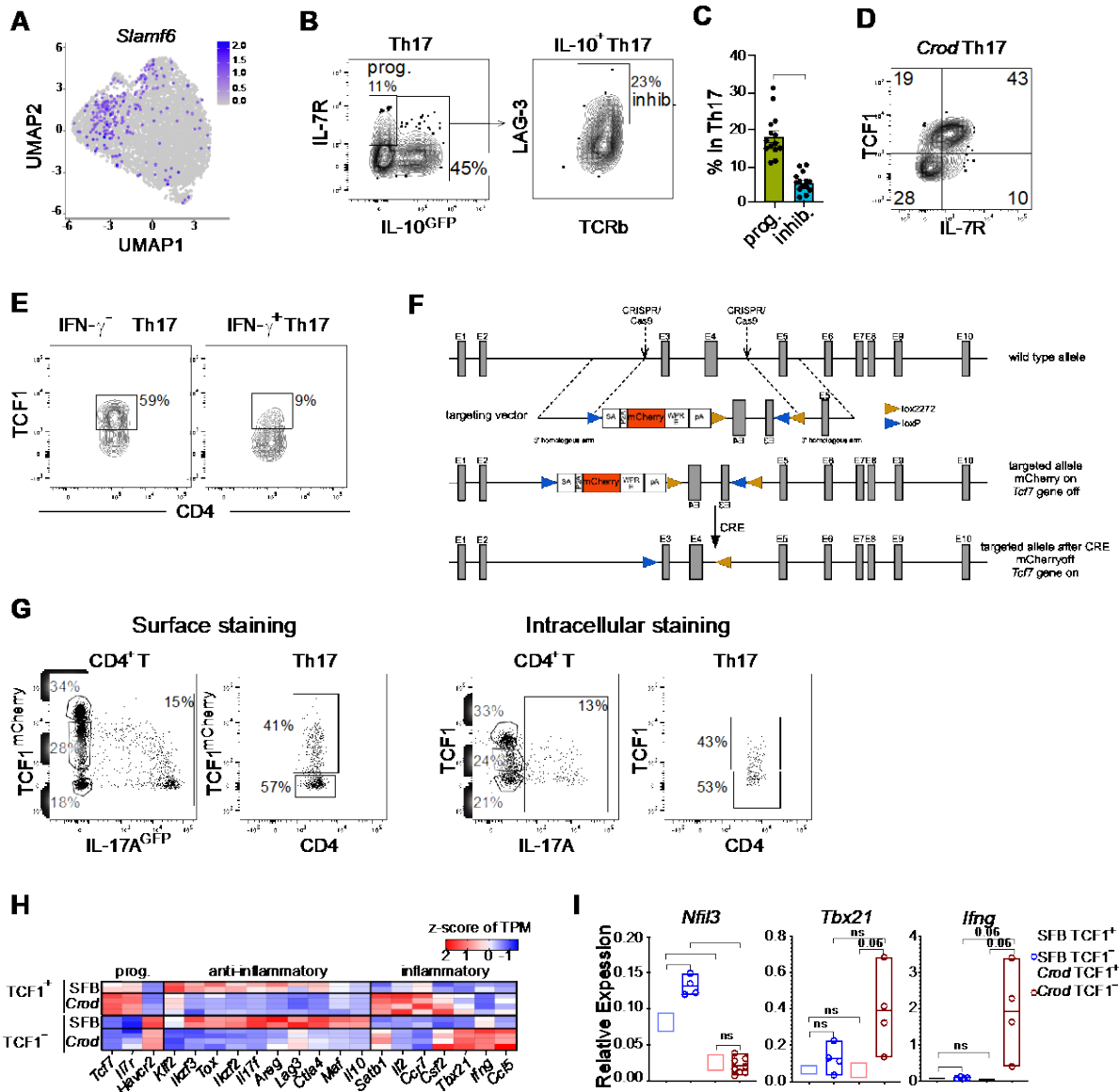


Figure S6. Commensal Th17 cells contain a progenitor TCF1⁺ population. Related to Figure 6

(A) Expression of *Slamf6* mRNA in individual SFB SI LP Th17 cells in the UMAP clustering in Figure 5A. scRNA-Seq data from Th17 cells sorted from *Il10^{GFP}/Il17a^{Katushka}/Foxp3^{mRFP}* mice.

(B) Gating scheme for purification of SFB progenitor and inhibitory Th17 cells from SI LP of *Il10^{GFP}/Il17a^{Katushka}/Foxp3^{mRFP}* mice. Left gated on TCRβ⁺CD4⁺Foxp3^{mRFP}-IL-17^{Katushka}⁺ lymphocytes.

(C) Proportions of the two subsets in (B) within SI LP Th17 cells.

(D) TCF1 and IL-7R expression in LI LP Th17 cells from *Crod*-infected mice at Day 14. Gated on TCRβ⁺CD4⁺IL-17⁺ lymphocytes.

(E) TCF1 expression in IFN-γ⁻ and IFN-γ⁺ LI LP Th17 cells from *Crod*-infected *Il10^{GFP}/Il17a^{Katushka}/Foxp3^{mRFP}* mice. Two independent experiments.

(F) Targeting strategy for generation of *Tcf7^{mCherry}* reporter mice (details in Methods).

(G) Representative FACS plots of SI LP CD4⁺ T cells in *Tcf7^{mCherry/+}/Il17a^{GFP/+}* double reporter mice and corresponding intracellular staining of the same sample. Plots gated on CD4⁺ LP T cells.

(H) Expression of select progenitor, anti-inflammatory, and pro-inflammatory genes in RNA-Seq of TCF1⁺ and TCF1⁻ Th17 cells from SI LP of SFB-colonized and LI LP of *Citrobacter rodentium*-infected (*Crod*) mice. One experiment, n = 2-4 mice/group.

(I) Quantitative PCR in FACS-purified TCF1⁺ and TCF1⁻ Th17 cells from SI LP of SFB-colonized or LI LP of *Crod*-infected mice. Two independent experiments, n = 4-6 mice/group.

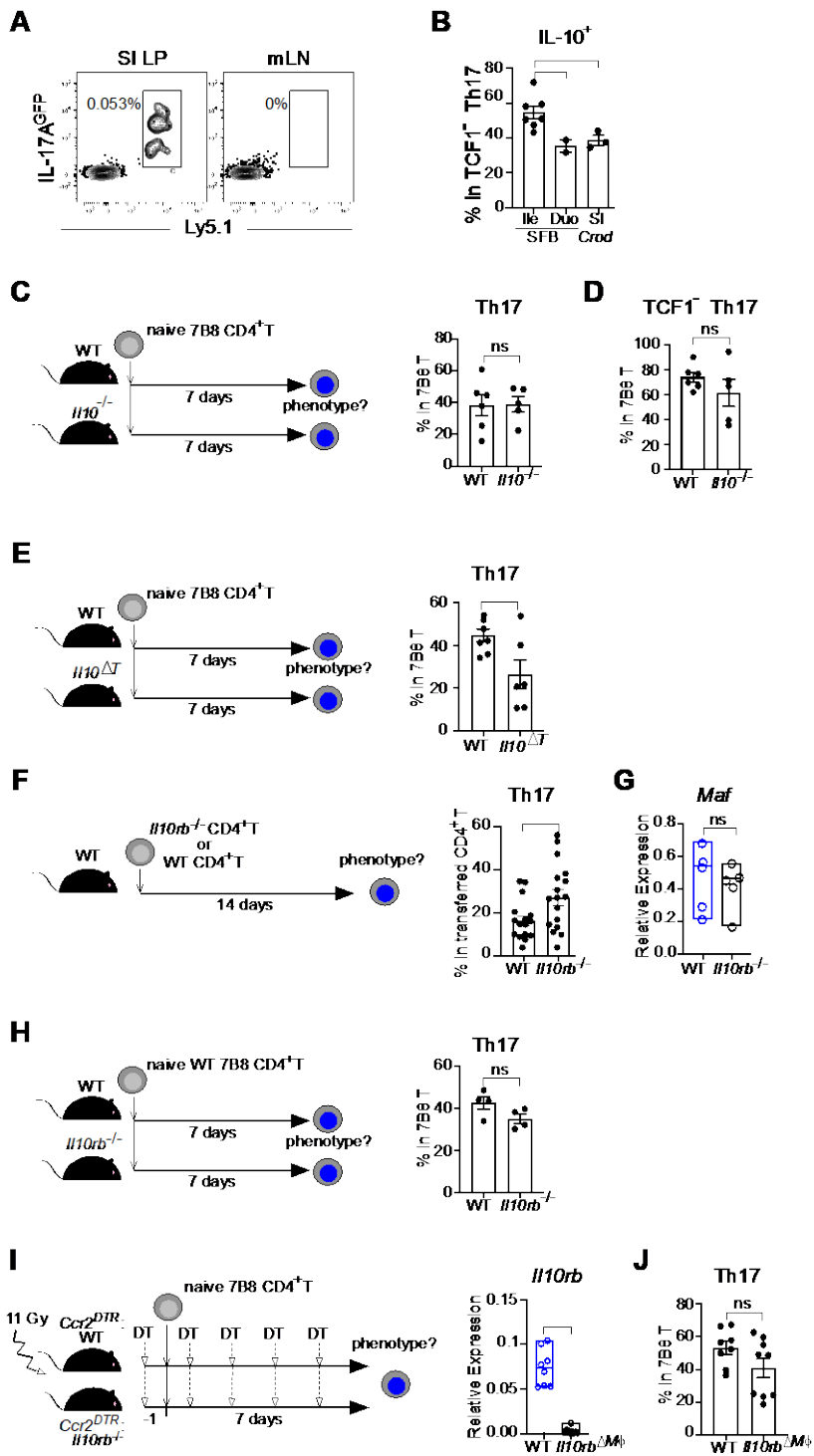


Figure S7. IL-10 signaling in intestinal M ϕ drives IL-10 expression in SFB Th17 cells.

Related to Figure 6

(A) TCF1^{mCherry+}IL-17^{GFP+} Th17 cells were FACS-purified from SI LP of SFB-colonized Ly5.1 double reporter mice and adoptively transferred into WT Ly5.2 recipients. Frequency and phenotype of transferred cells was examined two days later in mLN and SI LP. Plots gated on TCR β ⁺CD4⁺ lymphocytes.

(B) TCF1^{mCherry+}IL-17^{GFP+}IL-10^{Venus-} Th17 cells were FACS-purified from SI LP of SFB-colonized or *Crod*-infected mice and stimulated *in vitro* as described in Methods for 4 days. Three independent experiments, n = 2-7 mice/group.

(C, D) Frequency of SI LP 7B8 Th17 cells and TCF1⁻ 7B8 Th17 cells 7 days after transfer of naïve 7B8 triple reporter CD4⁺ T cells into SFB-colonized WT and *Il10*^{-/-} mice. Cumulative of three independent experiments, n = 5-6 mice/group.

(E) Frequency of SI LP 7B8 Th17 cells 7 days after transfer of naïve 7B8 triple reporter CD4⁺ T cells into SFB-colonized WT and *Il10*^{ΔT} mice. Cumulative of two independent experiments, n = 6-7 mice/group.

(F) Frequency of SI LP Th17 cells within transferred CD4⁺ T cells 14 days after transfer of naïve WT or *Il10rb*^{-/-} triple reporter CD4⁺ T cells into SFB-colonized WT mice. Cumulative of several independent experiments, n = 15-17 mice/group.

(G) Naive Ly5.2 WT or *Il10rb*^{-/-} CD4⁺ T cells from triple reporter mice were adoptively transferred into SFB-colonized WT Ly5.1 congenic recipients. Two weeks later transferred T_H17 cells (Ly5.2⁺TCR β ⁺CD4⁺Foxp3^{mRFP}-IL-17^{Katushka+}) were FACS-purified from SI LP and *Maf* expression assessed by quantitative PCR. Cumulative of several independent experiments, n = 5 mice/group.

(H) Frequency of SI LP 7B8 Th17 cells 7 days after transfer of naive 7B8 triple reporter CD4⁺ T cells into SFB-colonized WT and *Il10rb*^{-/-} mice. Cumulative of two independent experiments, n = 4 mice/group.

(I) Quantitative PCR of *Il10rb* transcript expression in FACS-purified sorted SI LP Mφ (CD11c⁺MHCII⁺CD64⁺) from WT and *Il10rb*^{ΔMφ} mixed bone marrow chimeras following DT treatment. Cumulative of several independent experiments, n = 5-8 mice/group.

(J) Frequency of Th17 cells in SI LP within transferred Ly5.1⁺ CD4⁺ T cells one week after transfer into WT and *Il10rb*^{ΔMφ} mixed bone marrow chimeras.